EXAMINING THE CONTRIBUTION OF THE DNA DAMAGE RESPONSE TO
SEPSIS SURVIVOR MYELOSUPPRESSION

by

Laura A. Huff

A thesis submitted to the faculty of
The University of North Carolina at Charlotte
in partial fulfillment of the requirements
for the degree of Master of Science in
Biology

Charlotte

2020

Approved by:

_____
Prof. Mark G. Clemens

_____
Prof. Didier Dréau

_____
Prof. Ian Marriott

ABSTRACT

LAURA A. HUFF. Examining the contribution of the DNA damage response to sepsis survivor myelosuppression. (Under the direction of MARK G. CLEMENS)


A large portion of patients who survive sepsis, a life-threatening hyperinflammatory response to infection resulting in organ dysfunction, experience a higher risk of mortality than non-septic patients. Innate immune cells of sepsis survivors exhibit a reduced ability to differentiate into a pro-inflammatory phenotype, and many sepsis survivors are unable to mount an adequate immune response to subsequent infection. Based on evidence that sepsis causes increased production of reactive oxygen (ROS) and nitrogen (RNS) species in innate immune cells, which leads to oxidation and injury to DNA and subsequent up-regulation of the DNA damage response (DDR), and on evidence of interplay between the DDR and the immune response in regulating cellular homeostasis, we proposed that factors involved in the DDR play a mechanistic role in triggering the epigenetic change in innate immune cells that leads to this myelosuppression. We hypothesized that constituents of the DDR play a causal role in initiating the epigenetic changes that occur in myeloid stem and progenitor cells (HSPCs) during sepsis and resulting in the persistent macrophage tolerance during subsequent infection. In a cecal ligation and puncture (CLP) murine model of sepsis, our data indicates that bone marrow derived macrophages (BMDMs) from septic mice demonstrate a reduced ability to exhibit the pro-inflammatory 'M1' phenotype, as evidenced by several phenotypic markers including iNOS protein expression, nitric oxide (NO) production, and cell morphology. We have further determined that a specific concentration range of glucose oxidase (GOx),

a source of oxidative stress, may mimic this phenotypic hypo-responsiveness in BMDMs and RAW 264.7 cells and cause increased activation of DNA damage response (DDR) factor ATM. These results suggest a role for DDR factors in macrophage immunosuppression in sepsis survivors.
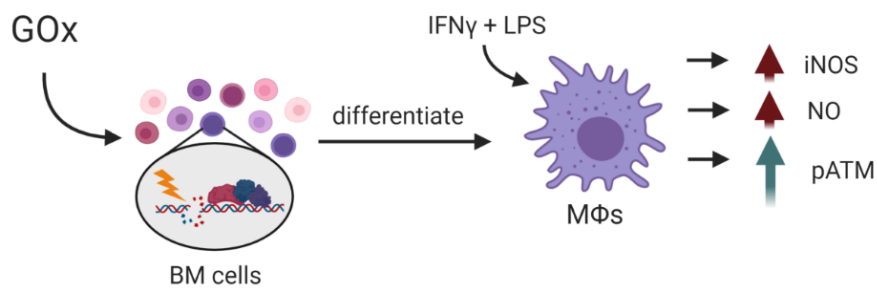
GRAPHICAL ABSTRACT

LAURA A. HUFF. Examining the contribution of the DNA damage response to sepsis survivor myelosuppression. (Under the direction of MARK G. CLEMENS)

Sepsis leads to suppression of the M1 phenotype and increased DDR in MΦs *in vivo*

IFNγ + LPS

Sepsis

differentiate

Survivor BM cells   Survivor MΦs

iNOS
NO
M1 morphology
pCHK1
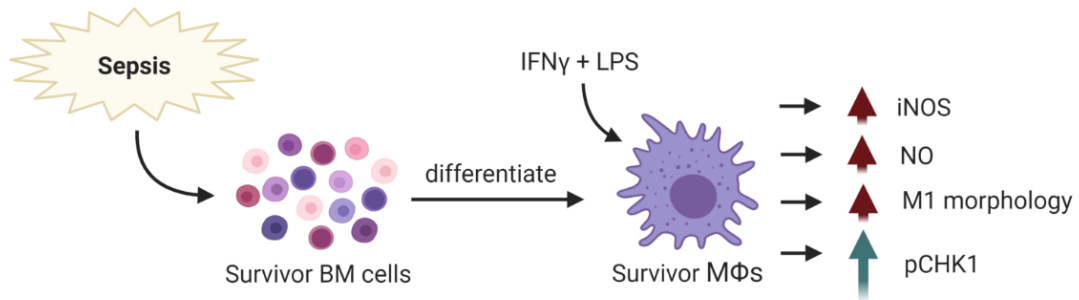
GOx leads to suppression of the M1 phenotype and increased DDR in MΦs *in vitro*

GOx

IFNγ + LPS

differentiate

BM cells   MΦs

iNOS
NO
pATM

Our data indicate that both sepsis and glucose oxidase (GOx) suppress macrophage M1 phenotype and promote the activation, i.e. phosphorylation, of key DDR proteins: Chk1 and ATM. Red arrows indicate suppressed expression while green arrows indicate increased expression. Figure generated using Biorender.com

DEDICATION

I dedicate this thesis to my mom, Pamela, for her unwavering support of all my academic

pursuits and inspiring in me a love of science at a very early age. I would never be

where I am today without her.

TABLE OF CONTENTS

LIST OF TABLES

LIST OF FIGURES

CHAPTER 1: INTRODUCTION

Sepsis is a state of life-threatening organ dysfunction that occurs due to dysregulated and excessive host response to an infection.[1] Greater than 1.7 million adults in the U.S. and 30 million people worldwide develop sepsis each year. In the U.S., approximately 270,000 people die from sepsis.[2] Treatment costs are among the highest for any disease at approximately $23.6 billion and increasing by 11.5% each year since 2013.[3] The pathophysiology is complex and a myriad of factors contribute to its development. Sepsis also presents with a wide array of symptoms such as hypoxia, hypotension, hypercoagulation, circulatory failure, tachycardia, high blood lactate levels, metabolic disorders, and multiple organ failure (MOF).[1,3] Advances in emergency medical care have produced a steep rise in the number of patients who survive sepsis in recent years. However, a large portion of sepsis survivors face long-term complications including physical, psychological, and cognitive disorders, as well as persistent immunological impairment and immunosuppression associated with a lifelong increased risk of mortality. The reasons for this increased rate of mortality among sepsis survivors is thought to be due to changes in their innate immune system function, resulting in immune dysregulation and inability to respond adequately to subsequent infection. Dysregulation of the innate immune function in sepsis survivors is termed the persistent inflammation, immunosuppression, and catabolism syndrome (PICS). The mechanisms underlying this immunosuppression remain unclear and are the subject of intensive research.[4]

It was thought previously that in the septic patient, the innate immune system initially responds to infection to an exaggerated extent, triggering successive immunosuppression. An initial massive hyper-inflammatory response to eliminate the

pathogen(s) leads to systemic activation of innate immune cells and circulation of cytokines, often referred to as a "cytokine storm". Within hours, a compensatory hypo-inflammatory response is mounted to initiate tissue repair due to tight regulation of the innate immune system to prevent extensive host damage.[5] The hyper-inflammatory phase is characterized by increased oxygen consumption, elevated ATP production, a metabolic switch to aerobic glycolysis (the Warburg effect), increased catabolism, and up-regulation of NADPH oxidase (NOX) and inducible nitric oxide synthase (iNOS) to produce antimicrobial reactive oxygen (ROS) and nitrogen (RNS) species. In contrast, the hypo-inflammatory response consists of decreased oxygen consumption, mitochondrial respiration, fatty acid oxidation (FAO), and tolerance of immune cells to pathogenic threats.[6-7] The hypo-inflammatory phase was viewed as a protective response to initial hyper-inflammation and oxidative damage to tissues by ROS and RNS secreted by activated innate immune cells and termed the compensatory anti-inflammatory response syndrome (CARS). Hyper- and hypo-inflammation, may occur simultaneously.[8] Regardless, after recovery the physiological symptoms of sepsis survivors are typically that of immuno-impairment.[9]

The immunosuppression of innate immune cells in sepsis survivors is generally viewed as a form of "innate immune memory". Indeed, similarly to the adaptive branch of the immune system, recent studies have shown that innate cells are also capable of establishing memory. Innate immune memory is defined as a functional reprogramming of innate immune cells after an encounter e.g. with a pathogen, leading to either an enhanced (trained) or reduced (tolerant) response to subsequent encounters.[10] Macrophages, along with neutrophils, dendritic cells, T-helper (T_H) cells, and T-regulatory

(T_{reg}) cells play major roles in the immune response to sepsis and are one of the immune cells most impacted by immunosuppression.
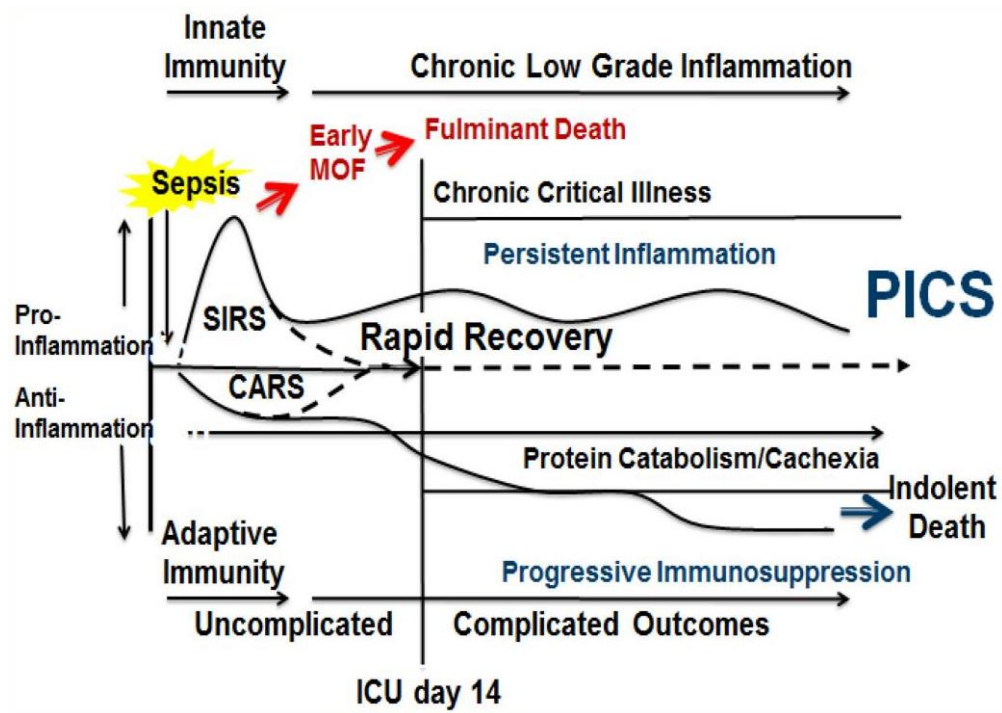
Figure 1. A model of the concurrent systemic inflammatory response syndrome (SIRS) and compensatory anti-inflammatory response syndrome (CARS) and the resultant persistent inflammation, immunosuppression, and catabolism syndrome (PICS).[8]

Phenotypic differences between macrophages from healthy individuals and those from sepsis survivors with impaired immune function (PICS) have been demonstrated.[11] Genes with inducible expression in macrophages under normal physiological conditions that are not inducible in 'tolerant' (Class T) macrophages include genes such as iNOS (NOS2), CD40, IL-6, IL-1β, caspase 12, etc. (for a list, see Table 1).[12]

Table 1. Proinflammatory and vasoactive genes not expressed in tolerant (Class T) macrophages and in 'non-tolerizeable' (Class NT) macrophages.[12]

Proinflammatory/Vasoactive

Function	Class T Gene	Class T Gene Name	Class NT Gene	Class NT Gene Name
proinflammatory	Cd40	CD40 antigen		
	Il6	interleukin 6		
	Il1b	interleukin 1 beta		
	Il12b	interleukin 12b		
	Il33	interleukin 33		
	Ptgs2	prostaglandin-endoperoxide synthase 2 (Cox-2)		
	Casp12	caspase 12		
vasoactive	Edn1	endothelin 1		
	Hdc	histidine decarboxylase		
	Lipg	lipase, endothelial		
	Nos2	nitric oxide synthase 2, inducible, macrophage		
procoagulation	F2r	coagulation factor II (thrombin) receptor	Fgl2	fibrinogen-like protein 2
	Serpine1	serine (or cysteine) peptidase inhibitor, clade E, member 1 (PAI-1)	F10	coagulation factor X
extracellular matrix	Mmp13	matrix metallopeptidase 13		
	Adamts4	a disintegrin-like and metallopeptidase (reprolysin type) with thrombospondin type 1 motif, 4		

Macrophages assume an array of phenotypes depending on the stimuli they are exposed to. This polarizability of macrophages upon stimulation is akin to the polarizability of T_H cells into Th1 or Th2 phenotypes. Macrophages are highly plastic and can assume phenotypes along a spectrum of various functional behaviors, where the extremes of the spectrum are: a pro-inflammatory M1 (classically activated) and anti-inflammatory M2 (alternatively activated) phenotype.[13] Notably, the genes that are not inducible in tolerant (T) macrophages are those associated with the M1 phenotype. Macrophages of sepsis survivors in both mice and humans have been shown to be unable to present the M1 phenotype upon stimulation with novel pathogen exposure or with a typical pattern recognition receptor (PRR) stimulant such as lipopolysaccharide (LPS), a

pathogen associated molecular pattern (PAMP) from the outer wall of gram-negative bacteria.[14-17] LPS is a major activator of toll-like receptor 4 (TLR4) on macrophages and the activation of TLR4 is one mechanism through which macrophage tolerance occurs.[12, 18] The phenotypic changes indicative of septic myelosuppression involve additional pathogen associated molecular pattern (PAMP)-associated signaling pathways and are not exclusive to chronic TLR activation.[4]

Epigenetic modifications such as chromatin remodeling, DNA methylation, noncoding RNAs, and histone methylation and acetylation play a major role in the induction of the myelosuppressive state in sepsis survivors.[4, 12, 19-24] Our knowledge of epigenetic regulation is still in its infancy, but chromatin modification is known to occur through DNA methyl transferases (DNMT), histone methyltransferases, histone acetyltransferases (HATs), histone deacetyl-transferases (HDACs), and non-coding RNA (ncRNA).[25] Class I, II, and IV HDACs are considered 'classical' HDACs that are Zn^{2+}-dependent metalloproteases while Class III HDACs, i.e., sirtuins, are NAD^+ dependent. Non-coding RNAs (ncRNAs) can bind directly to DNA (i.e. at enhancer or promoter sites, etc.) to prevent gene transcription or to mRNA transcripts to prevent translation.[4] HATs and HDACs have several additional non-chromatin targets that regulate processes such as metabolism and the cell cycle. Epigenetic regulation of chromatin is complex and can induce transient as well as stable, long-term modifications. Support for epigenetic contributions to myelosuppression include the demonstration that LPS stimulation can result in transcriptional silencing of several pro-inflammatory genes through the action of miRNAs.[21] Others showed that genes induced upon secondary stimulation in tolerant murine macrophages fall into two distinct categories: pro-inflammatory and anti-

microbial/metabolic genes. Epigenetic acetylation and methylation of histone 3 differentially regulate these changes.[12] Moreover, precise and selective chromatin modifications at promotor regions of inflammatory genes occurs in monocytes of human sepsis donors.[26] Lastly, hypo-responsiveness of the iNOS gene during myelosuppression is due to hypermethylation of CpG nucleotides and H3K9me methylation,[27] and demethylation of specific NF-κB responsive enhancer elements are associated with transactivation of iNOS.[28] These studies indicate that epigenetic modifications do occur during sepsis and can result in phenotypic changes including the hallmarks of myelosuppression such as the suppression of iNOS activation and of cytokine secretion by macrophages.

The mechanisms of macrophage tolerance and the associated epigenetic changes that occur remain to be elucidated. The pathogenesis of sepsis is highly complex and many signaling pathways are involved in the observed myeloid cell reprogramming. For example, activation of toll-like receptor 4 (TLR4) led to the same phenotypic changes in macrophages *in vitro* as detected in septic survivors. Activation of TLR4 has myriad downstream effects, for instance the activation of inflammasomes, which may contribute to the unresponsiveness of macrophages from septic individuals.[29] TLR4 activation in macrophages also increases endogenous reactive oxygen species (ROS) production. Here, we assessed the hypothesis that factors associated with the DNA damage response (DDR) are mechanistically involved in triggering the myelosuppressive state. This hypothesis is supported by two key findings: (1) the PARP1 inhibitor Olaparib confers beneficial effects to mice subjected to CLP sepsis[30], and (2) anthracyclines trigger ataxia telangiectasia mutated (ATM) activation, which is associated with 80% improvement in septic mouse

6

survival.[31] Both PARP1 and ATM are major regulators of the DNA damage response (DDR).[32] Additionally, the interplay between activation of the DDR and the innate immune response during infection is due to the major roles PARP1 and ATM play in innate immune cell homeostasis.[33]

ROS and RNS produced during the hyper-inflammatory phase of sepsis cause damage to nuclear DNA within innate immune cells and activate DDR pathways.[34] Initiation of the DDR signaling cascade activates numerous extensively studied proteins. Ataxia telangiectasia mutated (ATM) is a kinase that responds to double strand (ds) breaks. ATM is recruited to double-strand (ds) DNA breaks by the MRN protein complex. DDR foci uniquely contain γH2AX (phosphorylated histone H2A variant H2AX), which spreads throughout neighboring chromatin domains, nucleating additional response sites.[33, 35] Another protein involved in initiation of the DDR signal cascade is ataxia telangiectasia and Rad3 related (ATR), which is recruited to ss breaks and stalled replication forks. ATM and ATR are both also specifically linked to immune response regulation and maintenance of homeostasis following injury to DNA.[36]

We suggest that ATM is a critical DDR factor involved in epigenetic reprogramming of macrophages during sepsis. Indeed, ATM acts not only as a major regulator of DNA damage repair but also acts as an important redox sensor within cells.[35, 37] The majority of ATM is located in the nucleus of cells, but a fraction is also present in the cytoplasm where it may primarily act as a redox sensor. ATM is activated directly by oxidation and subsequently exists as an active dimer that does not require autophosphorylation. ATM also acts on a specific set substrates when activated by oxidation versus by DNA damage, resulting in different signaling pathways for each

stimulus.[37] One study has demonstrated that an ATM-AKT signaling pathway is triggered by cellular stressors, which can lead to induction of mitochondria-dependent apoptosis processes within the cell.[38] ATM also plays an important role in mitochondrial homeostasis through regulation of mitophagy.[39] It is possible that increased ATM activation through oxidation leads to increased autophagy and better sepsis outcomes. Interestingly, ATM-deficient mice exhibited hematopoietic stem cell (HSC) failure that was associated with a p16-retinoblastoma (Rb) stress pathway, which was preventable with anti-oxidant treatment.[40] This observation points to possible antioxidant effects downstream of ATM signaling. ATM is also essential in the self-renewal capacity of HSCs.[40] These studies support the hypothesis that signaling through ATM may contribute to the epigenetic changes that occur in hematopoietic stem and progenitor cells (HSPCs) during sepsis.

This study consisted of three AIMs: (1) to determine whether one or more phenotypic differences between sepsis survivors and healthy controls could be established in a mouse cecal ligation and puncture (CLP) murine model of sepsis, (2) to determine whether oxidative stress could replicate these phenotypic changes in a cell model, and (3) to determine whether the phenotypic changes due to oxidative stress, if found, are associated with DDR factors. For AIM I, bone marrow cells were collected from septic (mild and severe) survivors and non-survivors as well as healthy controls and differentiated into macrophages (BMDMs). The BMDMs were stimulated with a combination of LPS and IFN-γ (a potent M1 phenotype inducer) and assessed for phenotypic differences in iNOS expression and cell morphology. In AIM II we determined sublethal concentration ranges of glucose oxidase (GOx), a source of oxidative stress, that replicated phenotypic

changes found in the first AIM (i.e., iNOS expression) in several relevant cell models. In the last part of the study, AIM III, we used Western and dot blot analysis to determine whether phenotypic changes were associated with changes in activation of DDR proteins Chk1 and ATM.

CHAPTER 2: MATERIALS AND METHODS

Mouse CLP models of sepsis

The CLP model has been studied extensively and both the course of sepsis as well as the immune response are well-characterized in such mouse models.[41] The CLP model serves as a pre-clinical model given the ethical considerations in obtaining bone marrow cells from patients recovering from sepsis. We assessed two different experimental septic conditions: mild and severe levels of sepsis. Mild and severe sepsis conditions were achieved by administering antibiotics (carbapenum, 10 µL/g body weight) early (approximately 3 h post) or late (approximately 6-9 h post) after the CLP surgery procedure. Mouse temperature was monitored through an individual subcutaneous RFID transponder microchip implanted at least two days prior to CLP surgery. Mice were randomized to either the control or sepsis group prior to surgery and mice in the control and sepsis groups were housed in separate cages.

Cecal ligation and puncture (CLP) was performed under anesthesia (1-5% isoflurane) and following shaving and cleaning the abdomen area with alcohol and chlorhexidine. Analgesia was ensured through subcutaneous administration of Buprenorphine (0.1 mg/kg). Following a 1 cm laparotomy, the cecum was exteriorized, ligated with a silk suture and punctured twice with a 22-gauge needle. After replacement of the cecum into the peritoneum, the incision was closed using sutures. Control mice were operated with sham surgery conducted with all the steps listed for experimental animals except the puncture of the cecum. The mice were administered fluids (~1.2 mL of sterile saline), returned to their cages, kept on a warming pad, and monitored until they recovered

from the anesthesia. Antibiotic (carbapenum), analgesic (buprenorphine), and saline were given to the mice every 12 hours until they cleared the sepsis or reached the humane end point. These procedures were approved by the University IACUC (protocols # 17-008 and #20-006).

The temperature of the mice was monitored with the handheld RFID chip reader and recorded. We additionally scored the mice based on criteria approved by IACUC for reaching a humane endpoint (the 'sepsis score'). These two values (temperature and sepsis score) were recorded at each 12-hour check-in time point for each mouse. If a mouse reached the humane endpoint before the end point of the experiment (i.e. a 'non-survivor') the mouse was euthanized and tissue collection was conducted at that time. Euthanasia was conducted by transferring the mice to the Clemens Lab (Woodward 462), anesthetizing with isoflurane and collecting blood, resulting in euthanasia by exsanguination. Otherwise, mice were monitored until the end of the experimental window, at which point all remaining mice was euthanized. Experimental duration was between 3-21 days.

At the time of euthanasia, blood, femur and tibia bones, and tissue was collected. Blood was collected with a heparinized syringe ideally from the vena cava. Tissue from the liver, spleen, kidney, heart, and lungs were collected. Portions of each tissue were frozen in liquid nitrogen and stored at -80°C or stored in a 4% paraformaldehyde solution at 4°C for later analysis. Blood was separated by Ficoll separation to isolate PBMCs and portions were also centrifuged to separate out the plasma. The femur and tibia bones from the hind limbs were immediately isolated following blood and tissue collection. The bones may be stored in DPBS at 4°C for up to 24 hours before bone marrow cell isolation is

performed, but efforts were made to isolate bone marrow cells immediately following tissue collection.

Bone marrow cell isolation was conducted by removing the condyles from cleaned bones, centrifuging the bones at 10,000 RPM for 15 sec to allow red and yellow marrow to be extracted into centrifuge tubes. The red blood cells (RBCs) were lysed and the remaining cells was washed, counted and plated. The bone marrow cells were cultured in RPMI 1640 enhanced media containing supernatant from LADMAC cell culture media (containing macrophage colony stimulating factor 1, CSF-1, secreted by LADMACs) for at least 7 days for differentiation into macrophages.

Bone marrow derived macrophages (BMDMs) from each of the three resultant groups (septic survivors, septic non-survivors, and control mice) were plated for various experiments at a density of $0.5 - 1 \times 10^6$ cells/mL.

Cell culture

All cells were maintained in the incubator in a constant humidity environment, at 37°C, and 5% CO_2. The cell media contained the following ingredients except during treatments (i.e. with LPS + IFNγ), during which serum-free media was used. RAW 264.7 cells were cultured in Dulbecco's modified eagle medium (DMEM, Life Technologies 11965-092) supplemented with 10% heat-inactivated fetal bovine serum (FBS-HI, Serum Source FB02-500HI) and 2-5% penicillin-streptomycin (Life Technologies, 15140122). Murine bone marrow derived macrophages (BMDMs) were cultured in RPMI 1640 base media with L-glutamine (Life Technologies 11875093) supplemented with HEPES, 2-5% penicillin-streptomycin, LADMAC conditioned media (20%), and FBS-HI (10%). THP-1

and U937 cells were cultured in RPMI 1640 base media with L-glutamine (Life Technologies 11875093) supplemented with 10 mM HEPES, 2-5% penicillin streptomycin, 10% FBS-HI, 0.05 mM β-mercaptoethanol (Sigma Aldrich, M-3148), and 4.5 g/L D-glucose.

Cell treatments:

For experiments in which cells were treated with lipopolysaccharide (LPS) from *Escherichia coli* O26:B6 (Sigma Aldrich, L-3755) and recombinant interferon-γ (IFNγ) (from Abcam: human, ab9659 and mouse, ab9922), cells were incubated in a combination of LPS (0.001 mg/mL) and IFNγ (500-1,000 U/mL) for 20-24 h in serum-free media. For experiments in which cells were treated with glucose oxidase (10KU, Sigma Aldrich G2133), glucose oxidase concentrations were made up in serum-free cell media and cells were treated for 20-24 h. Cells were then washed two times with 1x DPBS and plated with cell media containing 10% FBS. Cells were then either differentiated into macrophages or experiments were conducted on undifferentiated cells, as indicated.

Griess reaction assay

In macrophages, nitric oxide (NO) is produced when iNOS is induced. Since iNOS is transcriptionally regulated, differences in NO production between stimulated septic (severe and mild) survivors, non-survivors, and control BMDMs will indicate differences in NO production specifically by iNOS. Nitrite levels were measured as an indication of nitric oxide (NO) production in cell media by first stimulating cells with a combination of lipopolysaccharide (LPS) and IFN-γ in serum-free media for 24 hours (0.001 mg/mL and 500-1,000 U/mL, respectively). Griess reagents consisted of a 4% sulfanilamide solution

and an 0.4% naphthylethylenediamene dihydrochloride solution, stored at 4 °C and protected from light. Nitrite standards were made from a stock 0.05 M sodium nitrite solution stored at 4 °C. Supernatant was dispensed into a 96-well plate and allowed to incubate with Griess reagents for approximately 20 minutes prior to plate reading the absorbance at 540 nm. Sample nitrite concentrations were extrapolated from a linear nitrite standard curve that included the test sample concentrations within the range of standards tested.

MTT cell viability assay

Cells were plated into a 96-well plate and allowed to incubate with various concentrations of glucose oxidase (GOx) for 20-24 h. MTT solution was added (20 µL) and allowed to incubate with the cells for 2 h at 37 °C. The supernatant was then carefully aspirated from each well and 150 µL of MTT solvent was added. Cells were rocked on a plate rocker for a total of 14 minutes and then the absorbance values were read by a plate reader at 590 nm.

Western blot

After the treatments of plated cells, the supernatant was removed from each well and ProPrep lysis buffer (Bulldog Bio, # 17081) was added (80 µL to 6-well plate wells and 40 µL to 12-well plate wells). Cells were scraped and allowed to incubate in the lysis buffer at -20 °C for 40 minutes prior to centrifugation at 13,000 RPM for 10 minutes at 4 °C and collection of the resultant supernatant into tubes for storage at -20 °C. Tissue homogenates were made by thawing 20-mg sections of tissue to 4 °C, adding 600 µL ProPrep lysis buffer (Bulldog Bio, 17081) per 10 mg tissue, homogenizing with a handheld

pellet mixer (VWR), passing the homogenized sample through a sterile 22 or 25 gauge needle, allowing the sample to sit in the -20 °C freezer for 20-30 minutes, then centrifuging at 13,000 x g and 4 °C for 2 min. Supernatant was collected and stored at -20 °C.

BCA assay analysis was performed using a Micro BCA Protein Assay Kit (ThermoFisher, PI23235) and bovine serum albumin (BSA, Sigma Aldrich, A7906) on all samples to determine the protein concentration. Samples were mixed with running buffer, Laemmli loading dye (BioRad, 161-0737), and β-mercaptoethanol (Sigma Aldrich, M1348) and boiled at 95 °C for 7 min. prior to loading into a polyacrylamide gel (7-8% resolving and 5% stacking layers) at a protein loading of 20-50 ng per well.   Gel electrophoresis was run at 75 V for 30 min., followed by 100 V for 1.5-2 h. Proteins were transferred to PVDF membrane (0.2 μm, ThermoFisher, #88520) by running the power supply at 350 mA for 1-2 h. PVDF membranes were blocked in 5% skim milk in 1x tris-buffered saline (TBS)-tween (1x TBST) at room temperature for 1 h or overnight at 4 °C. Primary antibody was allowed to incubate with the membrane overnight at 4 °C. Secondary antibody was allowed to incubate with the membrane for 1 h at room temperature, for 2-4 h at 4 °C, or overnight at 4 °C. The membrane was washed between each step three times for 5-15 minutes with 1x TBST. Membranes were incubated in enhanced chemiluminescent (ECL) substrate (WesternBright ECL HRP substrate, K-12045-D50, lot 170124-91) by mixing 400 μL of each substrate per membrane and adding the mixture dropwise or by additionally adding 2.5 mL DI H_2O to the mixture and adding directly to the lidded dish containing the membrane. Membranes were allowed to incubate in ECL substrate for 3-8 minutes, covered. Imaging was performed on a Bio Spectrum AC Imaging system.

Dot blot

After treating plated cells, adherent cells were scraped and the cell and supernatant mixture was centrifuged at 100 x g for 10 minutes. The supernatant was removed and stored at -80 °C. Cell pellets were resuspended in a 2:1 ratio of T-PER to ProPrep lysate buffers. Samples were sonicated in five to ten 1-second bursts and stored at -20 °C. The positive control for phospho-ATM (p-ATM) blots was made by adding 1 μM of camptothecin (CPT) to RAW 264.7 cells for 20 h. The RAW 264.7 cells were scraped, centrifuged at 150 x g for 10 min, 60 μL of ProPrep was added, samples were mixed via pipetting and sonication, and stored at -20 °C. BCA assay analysis was performed using a Micro BCA Protein Assay Kit (ThermoFisher, PI23235) and bovine serum albumin (BSA, Sigma Aldrich, A7906) on all samples to determine the protein concentration. Samples were mixed approximately 4:1:1 with 1x TBS Tween (TBST), 2.5% SDS, and sample, respectively and allowed to sit for 10 minutes prior to loading onto a 0.45-μm nitrocellulose membrane through the dot blotting apparatus. Samples were allowed to interact with the membrane for 15-30 minutes. Membranes were washed three times with 1x TBST prior to and after loading samples. Membranes were blocked with 5% skim milk in 1x TBST for 1 h at room temperature (RT) or at 4 °C prior to adding primary antibody. The membranes were rocked in primary antibody for 12-24 h at 4 °C, washed three times with 1x TBST, then rocked in secondary antibody for 2-12 h at 4 °C. The membranes were imaged using ECL substrate as described for Western blot analysis.

Microscope imaging

Cells were imaged in well plates, dishes, or flasks using an Olympus IX71 inverted fluorescence and phase contrast tissue culture microscope, Olympus TH4-100 external power supply, and Retiga EXi FAST IEEE 1394 FireWire[TM] digital CCD camera. The magnifications used are indicated by scale bars in each image. Fluorescent beads (1.0 μm) were incubated with BMDMs in the cell media for various periods of time (between 15-90 minutes). Media was then aspirated from each well or dish and the adherent cells were washed twice with DPBS. DPBS was then added to each well and cells were imaged using an Olympus FluoView FV500 laser scanning confocal microscope.

Statistical analysis

All data are presented as mean values ± standard error of the mean (SEM). Statistical analysis was performed using GraphPad Prism software (San Diego, California). Data were analyzed using two-way analysis of variance (ANOVA) testing for the Griess reaction assays, percentage of cells with pseudopodia, and phagocytosis of fluorescent bead experiments. Students t-test was used to analyze several of the Griess reaction assay results, as indicated in the figure captions. Pearson's correlation test was used to analyze the p-ATM dot blot results. p-values ≤ .05 were considered significant. Tukey's or Šídák's multiple comparison *post hoc* test was used between groups when statistical significance was detected.

CHAPTER 3: RESULTS

3.1 AIM I

Optimization of assays

A major study objective was to identify and develop a procedure to reliably detect one or more phenotypic change(s) that contributes to the inability of progeny macrophages from bone marrow (BM) cells of sepsis survivors to assume the proinflammatory 'M1' phenotype. Model RAW 264.7 and human mammary epithelial (HMEC) cell lines were used to optimize methods of inducible nitric oxide synthase (iNOS) expression detection through Western blot analysis and to measure nitric oxide (NO) production through a Griess reaction assay.
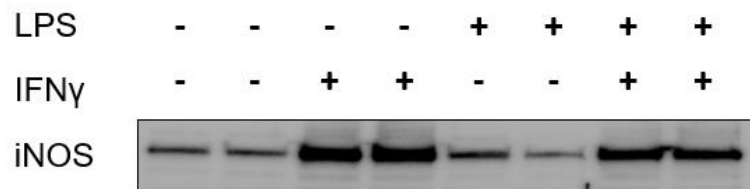
Figure 2: RAW 264.7 cells stimulated with IFNγ exhibit increased levels of iNOS expression. RAW 264.7 cells were subjected to Western blotting with iNOS antibodies after treating cells with various combinations of LPS (0.001 mg/mL) and mouse IFNγ (500 u/mL).

Western blot analysis of RAW 264.7 cells (Figure 2) indicated that cells stimulated with mouse IFNγ exhibit increased levels of iNOS expression. Interestingly, LPS did not appear to have an effect in causing upregulation of iNOS expression in RAW 264.7 cells.
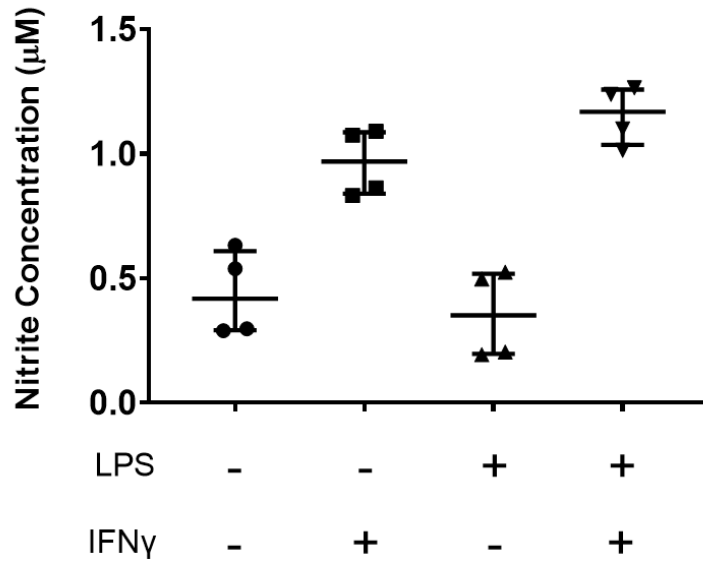
Figure 3: Stimulation of RAW 264.7 cells with LPS and IFNγ leads to increased nitrite production, an indicator of increased nitric oxide (NO) production. RAW 264.7 cells were incubated for LPS (0.001 mg/mL) and IFNγ (500 U/mL) for 22 h and nitrite levels were measured from the supernatant through Griess reaction assay analysis. One-way ANOVA analysis shows there is a significant effect of LPS and IFNγ treatment on the amount of nitrite produced by cells ($F_{3,4} = 25.05$, $p < .01$).

Preliminary Griess reaction assay results (Figure 3) indicate that RAW 264.7 cells stimulated with LPS (0.001 mg/mL) and IFNγ (500 U/mL) for 22 h produce a greater amount of nitric oxide than unstimulated cells. Tukey's HSD *post hoc* test shows that each group without IFNγ is significantly different than each group with IFNγ, although the groups with versus without LPS were not all different. This indicates that for RAW 264.7 cells and at the concentrations tested, stimulation with IFNγ plays a larger role than LPS in stimulating nitrite production.

Both Western blot analysis of iNOS as well as an indirect measurement of iNOS nitric oxide (NO) production, the Griess reaction assay, were successfully optimized for the RAW 264.7 cell line, which is a mouse macrophage line that shares many similarities

in morphology and responsiveness with mouse bone marrow derived macrophages (BMDMs).

Mild sepsis experiment

A mouse cecal ligation and puncture (CLP) model of sepsis was utilized. CLP sepsis has been demonstrated as a consistent and reliable source of sepsis in mouse models.[41] Both the course of sepsis as well as the immune response are well-characterized using this method.[42]

Sepsis was achieved by giving antibiotics within a relatively short time period (approximately 3 h) following the CLP surgery procedure. Bone marrow cells were collected from septic survivors and non-survivors as well as healthy controls and differentiated into macrophages (BMDMs). The macrophages were stimulated with LPS and IFN-γ because this combination is a well-known and potent initiator of differentiation to the M1 phenotype in mouse macrophages. The macrophages were then assessed for the aforementioned differences in activation of M1-associated phenotype(s). The first phenotype assessed for differential response was iNOS, which is regulated through transcriptional control of protein expression levels. Up-regulation was determined by two different methods, (1) iNOS protein expression levels through Western blot analysis and (2) nitric oxide (NO) production through a Griess reaction analysis. In macrophages, nitric oxide is produced when iNOS is induced. Thus, differences in NO production between stimulated septic survivors, non-survivors, and control BMDMs will indicate differences in NO production specifically by iNOS.

The mild sepsis experimental group consisted of eight mice (Table 2): three controls, one non-survivor, and four survivors.

Table 2: Number of mice in the control group as well as non-survivors and survivors in the sepsis group for the mild sepsis experiment.

Group	Number of mice
Controls	3
Sepsis Non-Survivors	1
Sepsis Survivors	4

Records of the sepsis score from the mice in the mild sepsis experiment (Figure 4) show that all of the mice in the septic group exhibited a higher highest score than any mice in the control group. Two mice had particularly high sepsis scores during the course of the experiment. However, the final scores of all septic group mice except one are extremely close to those in the control group. The one exception was the non-survivor, whose final sepsis score was higher than the rest of the mice in the septic group.
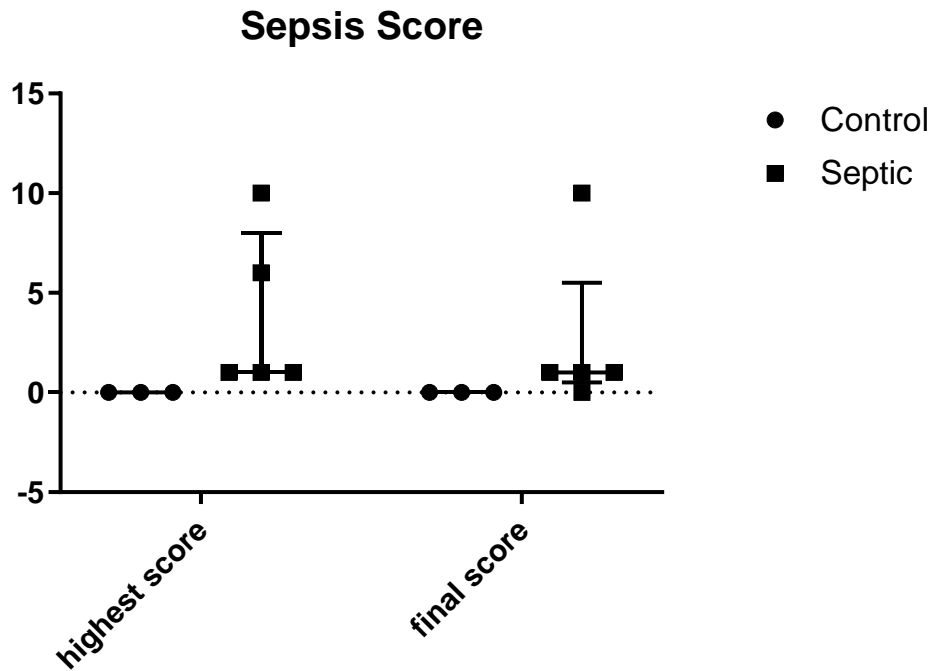
Sepsis Score

Figure 4: Highest and final sepsis scores of both control and septic mice in the mild sepsis experiment. The mouse with the highest score for both the highest total score and final score was the non-survivor.

The temperature of each mouse was monitored throughout the experiment using a hand-held sensor for the subcutaneous chips. A summary of the chip temperature data for the mild sepsis experiment (Figure 5) indicates that all mice had similar body temperatures at the beginning of the experiment. The control mouse temperatures were highly consistent throughout duration of the experiment, however the septic mice had larger variability in the lowest body temperature reached and reached lower temperatures than those in the control group. However, the final body temperatures of all the mice were similar with the exception of the one non-survivor.
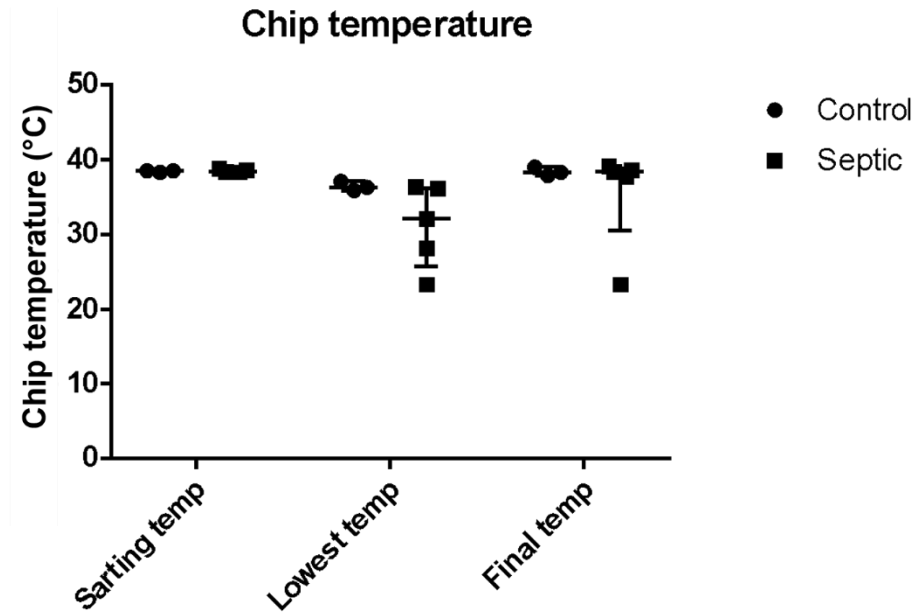
Figure 5: Starting, lowest reached, and final temperatures (°C) of the control and septic mice in the mild sepsis experiment. The lowest temperature reading in the final temperature grouping for the septic mice is the single non-survivor.

Bone marrow cells were cultured in LADMAC supernatant-containing media for seven days and either stimulated with LPS (0.001 mg/mL) and IFNγ (1,000 U/mL) for 24 h or left unstimulated. Griess reaction assay results of these cells show that unstimulated cells in both the control and septic groups do not exhibit high levels of nitrite production, as expected. Interestingly, there is a significant difference between the nitrite produced by stimulated cells in the septic group as compared to the controls where septic BMDMs produce significantly less nitrite than those in the control group ($p < .01$).
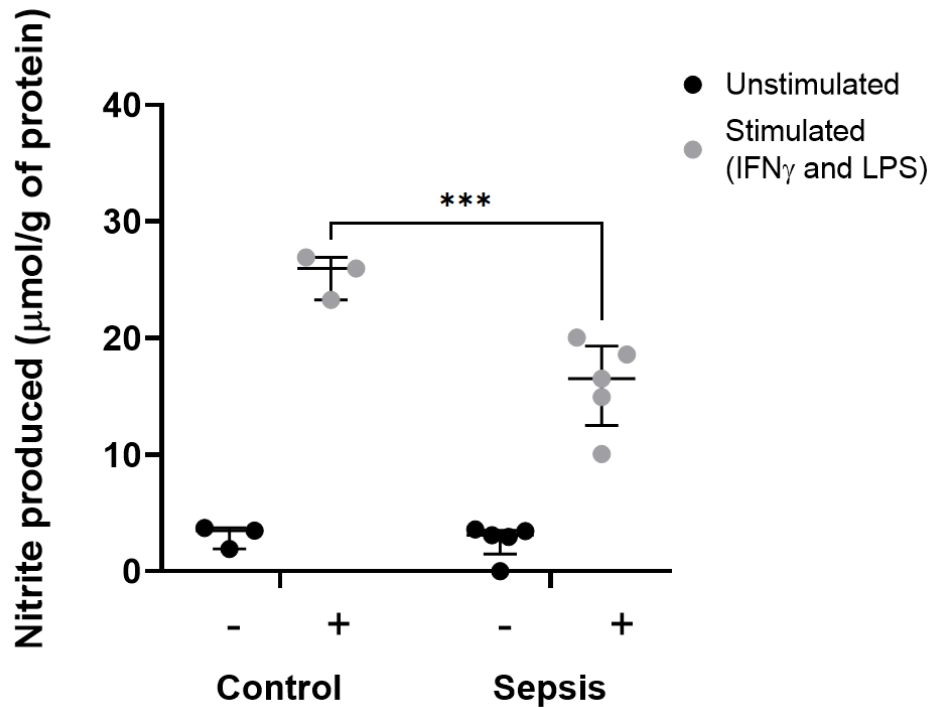
Figure 6: Nitrite produced by mouse bone marrow derived macrophages (BMDMs) from mice with mild sepsis. Cells were either stimulated with LPS (0.001 mg/mL) and IFNγ (1,000 U/mL) for 24 h or left unstimulated. A two-way ANOVA test shows a significant effect of sepsis ($p < .05$), stimulation ($p < .0001$), and the effect of sepsis on stimulation ($p < .05$). Tukey's *post hoc* test additionally shows a difference in nitrite production between the stimulated control and sepsis cells ($p = .0006$). ***$p < .001$.

Western blot analysis of iNOS expression from stimulated (with LPS + IFNγ) and unstimulated BMDMs of controls and septic mice in the mild sepsis experiment (Figure 7) exhibit a similar pattern as the Griess reaction results. Unstimulated BMDMs from controls and septic mice do not express detectable quantities of iNOS protein, as expected. However, stimulated septic mouse BMDMs express lower amounts of iNOS than control cells ($p < .001$). The one exception to this pattern in iNOS expression is the single non-survivor.
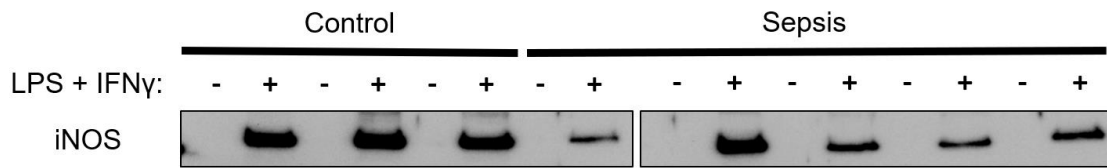
Figure 7: Western blot probing for iNOS protein in bone marrow derived macrophages (BMDMs) from control and septic mice in the mild sepsis experiment.

In addition to examining iNOS expression as an M1 phenotype indicator, morphological changes in the shapes of stimulated and unstimulated BMDMs were examined. One distinguishing morphological change observed was a greater number of projecting pseudopodia in certain conditions compared to others. The number of macrophages with projecting pseudopodia were counted and normalized to the total number of cells in microscope images (10x magnification) between unstimulated and stimulated control and septic groups. Extending pseudopodia are associated with anti-inflammatory 'M2' polarized macrophages ostensibly to clear apoptotic cells and other cellular debris.[43-44] Comparisons by way of a two-way ANOVA revealed no statistically significant differences between groups, however a general trend of a decrease in the percentage of cells with pseudopodia has occurred in the control BMDMs. The septic group demonstrated greater variability in the morphological response to stimulation. Some BMDMs in the septic group appear to follow the same trend as the control macrophages, while BMDMs from other subjects do not decrease to the same extent in percentage exhibiting pseudopodia with stimulation versus unstimulated and BMDMs from one subject display the opposite trend. Interestingly, the group of BMDMs that displayed the opposite trend are from the only non-survivor.

Individual Student's T-tests were conducted for the percentage of BMDMs with pseudopodia (Figure 8) results using the most conservative adjustment for multiple comparisons, multiplication of the p-value by a factor of two. In the control BMDMs, stimulation makes a difference in the percentage of cells exhibiting pseudopodia ($p = .053$); however, in septic BMDMs it does not. This is consistent with the Griess reaction results that indicate a significant change to the M1 phenotype upon stimulation. Control cells also exhibit a morphological shift toward displaying less pseudopodia upon stimulation, an indication of shifting into the M1 phenotype.[45] Greater variability occurs in the septic group.
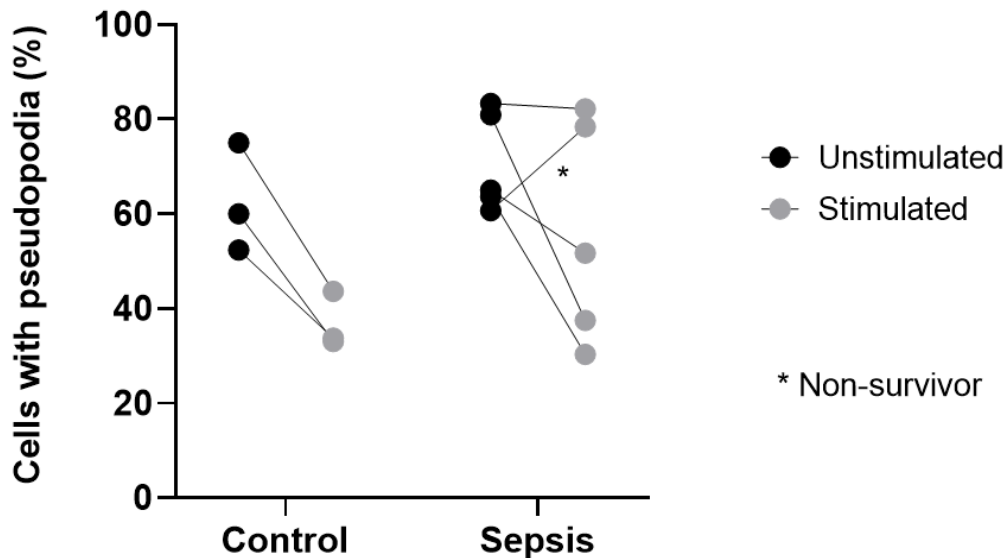
Figure 8: The percentage of bone marrow derived macrophages (BMDMs) with pseudopodia were determined from microscope images of cells cultured from all mice in the control and mild sepsis groups that were unstimulated or stimulated with LPS + IFNγ. Cells from the same subject are connected by lines. A two-way ANOVA shows no significant effect between the control (LS mean 49.6%) and sepsis (LS mean 63.4%) groups nor for the interaction between the condition of sepsis and stimulation. However, a significant effect was found between unstimulated (LS mean 66.6%) and stimulated (LS mean 46.4%) cells ($F_{1,12} = 6.12$, $p < .05$).

Severe sepsis experiment

Since the initial (i.e., mild) sepsis experiment resulted in only one non-survivor, we devised a second experiment to model a more severe form of sepsis. Severe sepsis was achieved by giving antibiotics 6-9 h post-CLP surgery to a group of five aged mice (approximately 24 months). The advanced aged of the mice is an important confounding variable to consider due to the likely effects on the results. The severe sepsis experiment consisted of only one control mouse due to surgical complications with the planned second control. The experiment resulted in all non-survivors (four) and no survivors.

Table 3: The severe sepsis experiment consists of one control mouse, four non-survivors, and zero survivors.

Group	Number of mice
Control	1
Sepsis Non-Survivors	4
Sepsis Survivors	0

The hind limb bones of the mice were highly brittle, which we believe is associated with the advanced age of the mice. The number of bone marrow cells obtained was substantially less than the number obtained during the initial (i.e. mild) sepsis experiment due to loss of bones to breakage. Additionally, a reduction in the number of red bone marrow (BM) cells per bone was observed, which is consistent with findings in mice of advanced age. Due to the low volume of cells obtained, portions of cell pellet material were unavoidably and inconsistently included in the Western blot samples. This

inconsistency led to an inaccurate BCA protein assessment and unequal protein loading into the gel, as indicated by the unequal amounts of actin loading control (Figure 9).
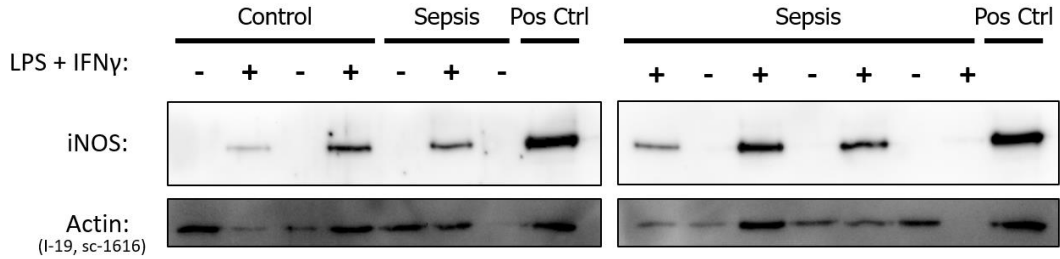
Figure 9: Western blot probing for iNOS and actin for control and septic mice in the severe sepsis experiment. The positive controls for iNOS are RAW 264.7 cells treated with LPS + IFNγ for 24 h. Due to low sample volumes, BCA analysis may have yielded incorrect results leading to unequal sample loading.

The BM cells were plated and cultured in LADMAC-containing media, differentiated into macrophages for seven days, and treated with the LPS + IFNγ combination. A Griess reaction assay was performed to measure the nitrite production of the stimulated and unstimulated cells (Figure 10). Two-way ANOVA statistical analysis shows that stimulation had an effect on nitrite production by the BMDMs ($p < .05$), however neither the condition of severe sepsis nor the effect of sepsis on the stimulation response showed a significant effect. While severe sepsis did not have a significant effect at the α level of 0.05, the p-value was notably close to 0.05 ($p = .068$). It is possible that with a greater number of subjects the effect of severe sepsis may be significant. The presence of only one control subject in this experiment has undoubtably also contributed to a lower statistical power for this analysis.
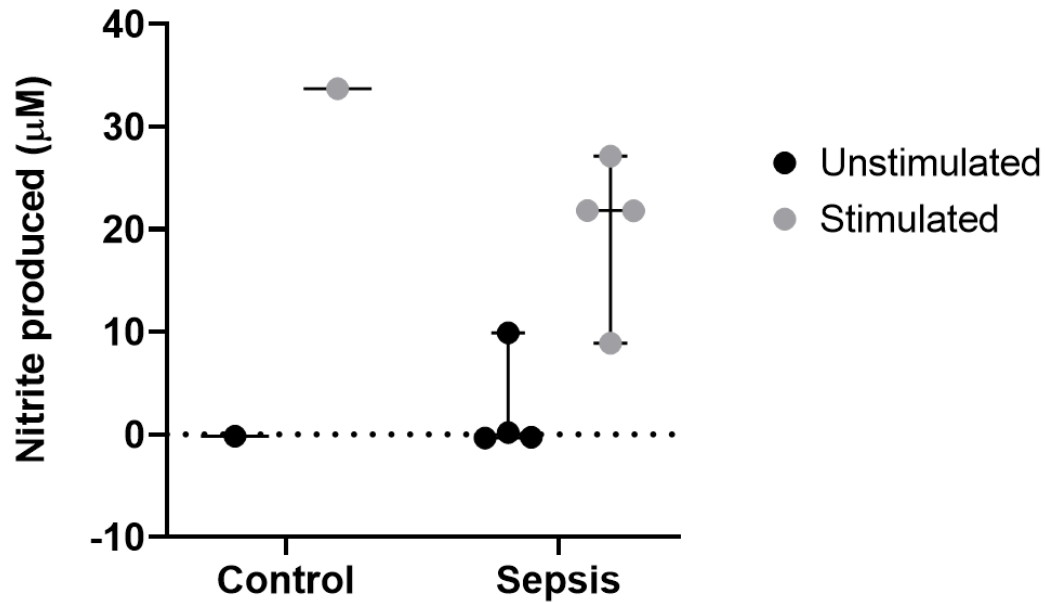
Figure 10: Nitrite production measured by Griess reaction assay analysis of BMDMs from mice in the severe sepsis experiment. Macrophages from the control and septic mice were stimulated with LPS + IFNγ (0.001 mg/mL and 1,000 U/mL, respectively) or left untreated for 24 h prior to nitrite measurements. Two-way ANOVA analysis with repeated measures for each mouse shows that stimulation does have a significant effect on the nitrite production ($F_{1,3} = 13.35$, $p < .05$). Severe sepsis did not have a significant effect at the alpha level of 0.05, however the p-value was notably close to 0.05 ($F_{1,3} = 7.88$, $p = .068$). The effect of sepsis on stimulation was also found not to be significant ($F_{1,3} = 1.35$, ns).

Another marker associated with differences between M1 and M2 macrophage phenotypes is phagocytic ability. Previous studies have shown that incubation of BMDMs with M2-promoting cytokines such as IL-4 and IL-10 result in macrophages with higher engulfment of particles than M1-polarized macrophages.[46] Here, BMDMs were plated into four-section confocal dishes and incubated with green fluorescent 1.0-μm beads for 0, 15, 30, or 60 minutes, washed, and imaged with a confocal microscope (Figure 11). While no statistically significant differences were found between the groups, general trends were observed. Results from the $t = 60$ min. time point (Figure 12) indicate that when control BMDMs are stimulated they may engulf more beads than unstimulated macrophages ($p =$

ns). This is in contrast to the general trend observed in the septic group, where stimulation of BMDMs may result in a lower number of engulfed beads. This trend also appears to be contradictory to the Griess reaction analysis results, which showed that the stimulated control BMDMs exhibit greater iNOS expression markers, indicating a shift to the M1 phenotype (if consistent with literature data). The bead phagocytosis study appears to indicate that the stimulated BMDMs exhibit a greater extend of bead phagocytosis, which is usually indicative of the M2 phenotype. However, it is possible that various M2 sub-phenotypes behave differently with respect to phagocytic ability. It is also possible that macrophages from septic mice assume a phenotype that is not classically M1 or M2, but may be a separate sub-phenotype.
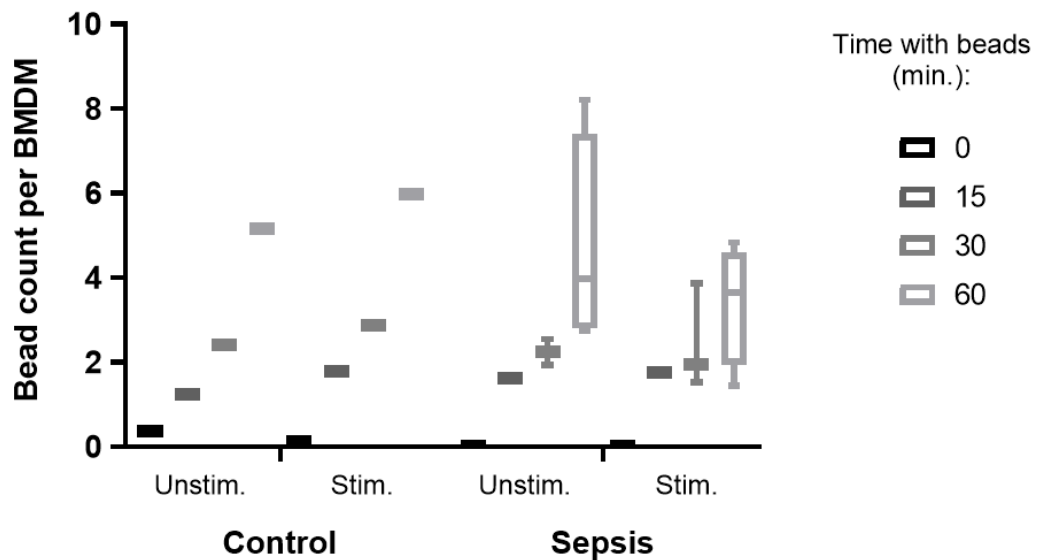
Figure 11: Phagocytosis of fluorescent green 1-μM beads by mouse BMDMs in the control and sepsis group of the severe sepsis experiment. Cells were incubated with beads for different periods of time (0-60 min.).
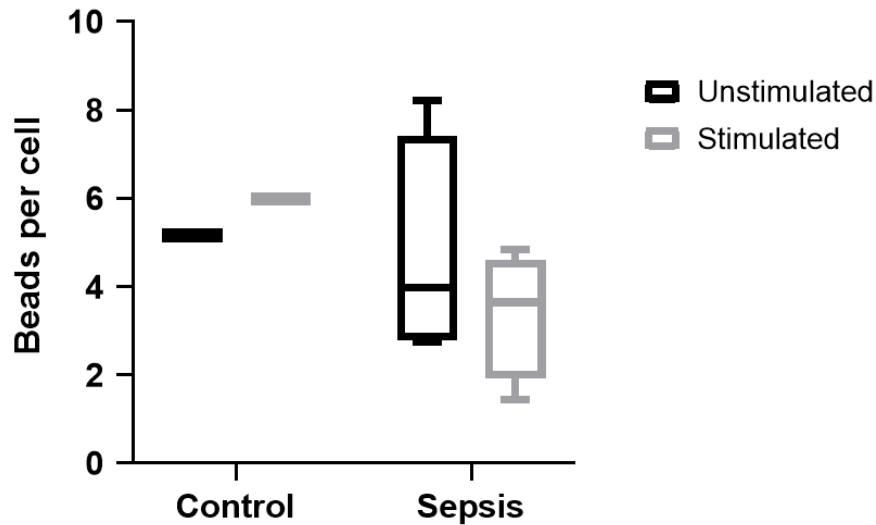
Figure 12: Phagocytosis of fluorescent green 1-µM beads by mouse BMDMs in the control and sepsis group of the severe sepsis experiment. Cells were incubated with beads for 60 min. A two-way ANOVA analysis showed no significant differences between stimulated and unstimulated cells nor between control and sepsis groups or the interaction between the two factors ($F_{1,3} = 0.58$, ns).

Aged controls

The bone marrow cells of three aged mice were harvested and plated for experiments to use as additional controls for the severe sepsis experiment due to the presence of only a single control mouse in this study. The Griess reaction assay results obtained after stimulating the macrophages with LPS + IFNγ or leaving the cells unstimulated were graphed alone (Figure 13) and with the severe sepsis experiment Griess reaction assay results (Figure 14). These results are considered comparable due to the similarity in age and use of the same breed of mice. Addition of the aged control subject data to the severe sepsis experiment data resulted in a significant effect of both severe sepsis ($p < .01$) and stimulation ($p < .001$). The interaction between sepsis and stimulation was not found to be significant. These additional data points increased the statistical power

31

of the Griess reaction analysis and yielded more information about significant factors in

nitrite production of the BMDMs.
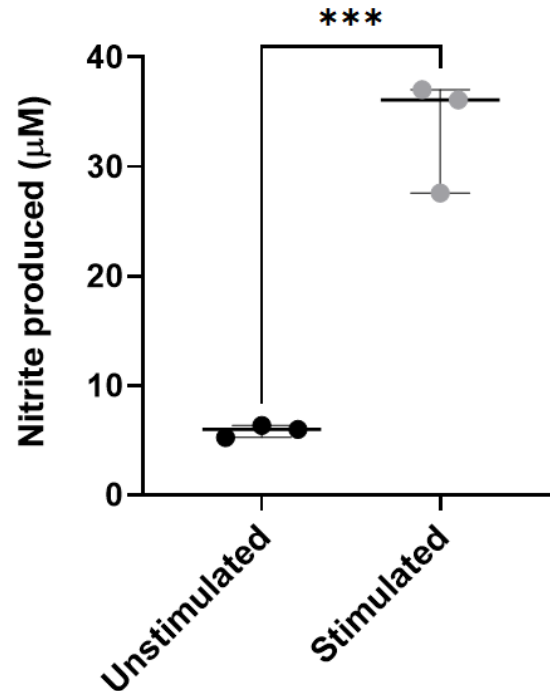
Figure 13: Aged control mouse Griess reaction results alone. Nitrite produced in three aged control mouse bone marrow derived macrophages (BMDMs) unstimulated and stimulated with LPS + IFNγ measured by Griess reaction assay analysis. Median nitrite values with 95% confidence intervals are shown. Student's t-test analysis indicates a significant difference between the unstimulated (mean = 5.87, SD = 0.56) and stimulated (mean = 33.58, SD = 5.20) groups (t = 9.184, df = 4, p = .0008). ***$p < .001$.
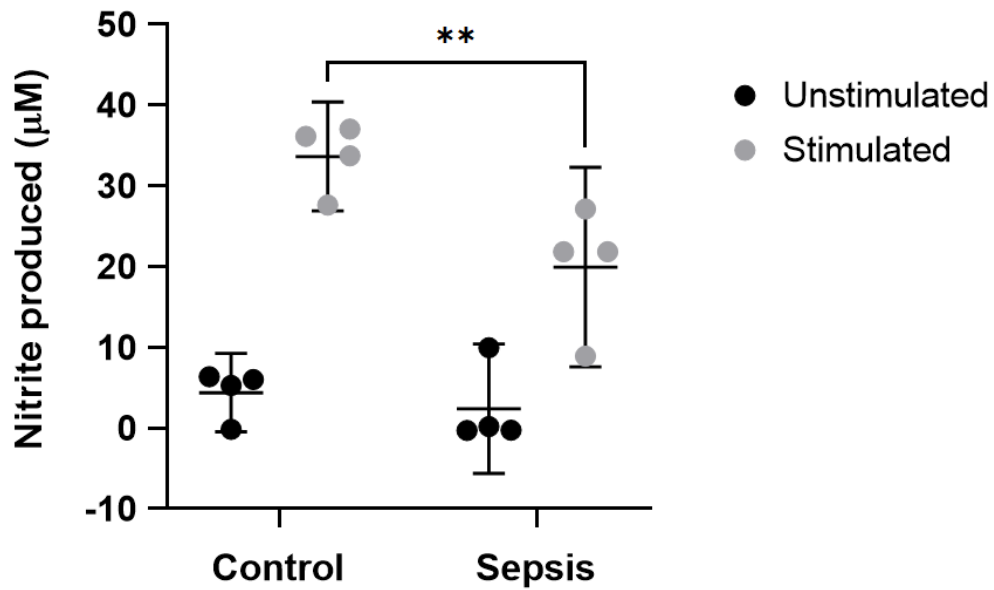
Figure 14: Nitrite production measured by Griess reaction assay analysis of BMDMs from mice in the severe sepsis experiment with three additional aged control mice. Macrophages from the control and septic mice were stimulated with LPS + IFNγ (0.001 mg/mL and 1,000 U/mL, respectively) or left untreated for 24 h prior to nitrite measurements. Two-way ANOVA analysis with repeated measures for each mouse shows that both severe sepsis ($F_{1,6} = 26.81$, $p < .01$) and stimulation ($F_{1,6} = 46.31$, $p < .001$) have a significant effect on the nitrite production. The interaction between sepsis and stimulation was not found to be significant ($F_{1,6} = 2.90$, ns). Šídák's *post hoc* test shows there is a difference in nitrite produced by stimulated control versus septic cells ($p = .0067$). **$p < .01$.

3.2 AIM II

The first goal of AIM II was to determine a sublethal source of oxidative stress that will trigger the DNA damage response in a macrophage cell model. More specifically, we sought to determine whether the phenotypic changes observed in AIM I between septic mice and controls, such as differences in iNOS upregulation in response to stimulation (with LPS + IFNγ), could be replicated in an *in vitro* cell model of sepsis. Glucose oxidase (GOx) was used as a source of oxidative stress to initiate DNA damage repair processes.

Glucose oxidase (GOx) is an enzyme that uses oxygen to catalyze the oxidation of α-D-glucose to hydrogen peroxide (H_2O_2) and D-glucono-δ-lactone. When GOx is added to cell culture media the enzyme utilizes oxygen and glucose in the media to produce H_2O_2 proportional to the activity of GOx added. Hydrogen peroxide is a major source of oxidative stress to cells and has been shown to induce cellular injury such as DNA damage in a dose-dependent manner.[47] Glucose oxidase was therefore used to induce oxidative stress in multiple mouse and human monocyte/macrophage cell types to establish a cell line with reproducible and detectable levels of nitrite in response to LPS + IFNγ stimulation.

To determine whether there is a sublethal range of GOx concentrations that induces a DDR, MTT cell viability tests were conducted for each different cell type. The MTT cell viability assay of human mammary epithelial cells (HMECs) treated with different concentrations of GOx (0 to 3 U/mL) for 24 h indicates that these cells begin undergoing cell death between 0.003 and 0.03 U/mL GOx (Figure 15).
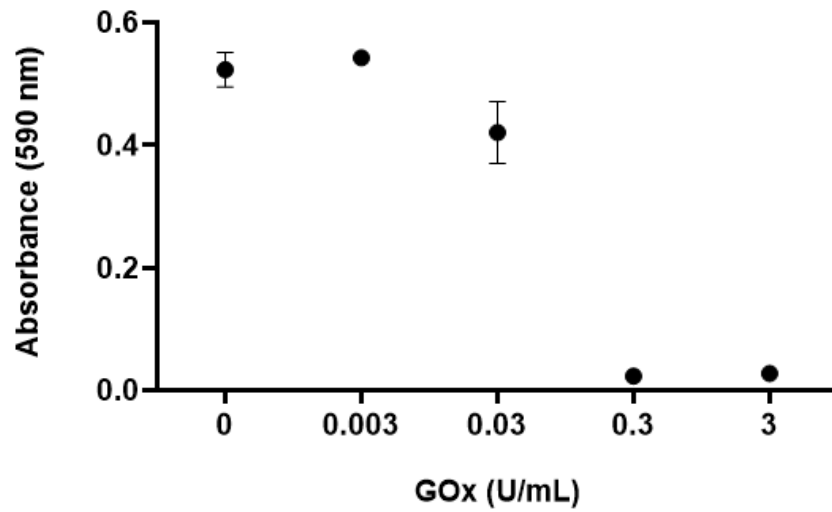
Figure 15: MTT cell viability assay of human mammary epithelial cells (HMECs) treated with different concentrations of GOx (0 to 3 U/mL) for 24 h. Mean values and SEM are indicated with bars.

The MTT cell viability assay of human monocytic THP-1 cells (a cell line from a male 1-year-old leukemia patient) treated with different concentrations of GOx (0 to 0.3 U/mL) for 24 h indicates that the THP-1 cells begin undergoing cell death between 0 and 0.0125 U/mL GOx (Figure 16).
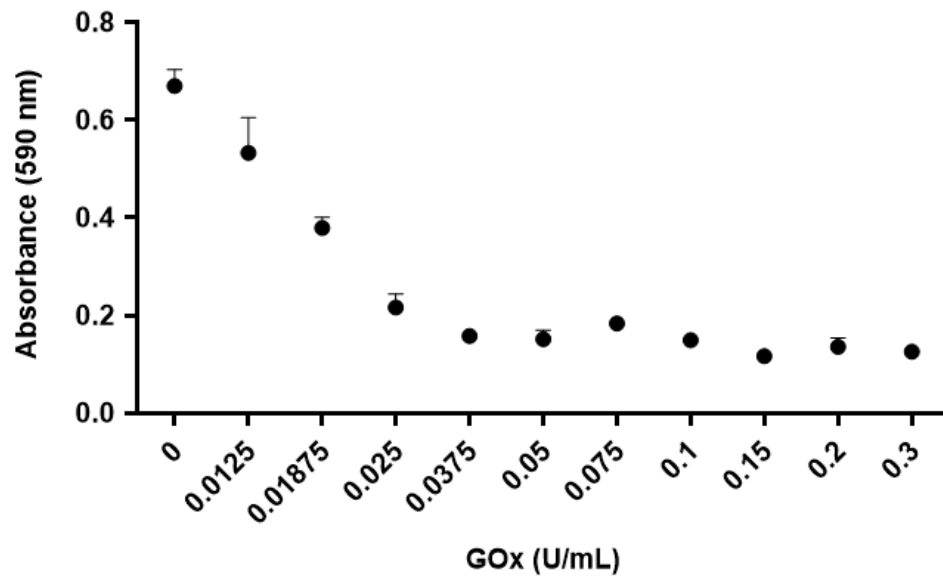
Figure 16: MTT cell viability assay of human THP-1 cells differentiated into macrophages and treated with different concentrations of GOx (0 to 3 U/mL) for 24 h. Mean values and SEM are indicated with bars.

The MTT cell viability assay of human monocytic U937 cells (a cell line originally derived from a 37-year old male lymphoma patient) treated with different concentrations of GOx (0 to 0.3 U/mL) for 24 h indicates that the U937 cells begin undergoing cell death between 0.0125 and 0.01875 U/mL GOx (Figure 17). The U937 cells appear to be slightly less sensitive to the GOx treatment than the highly similar THP-1 cells.
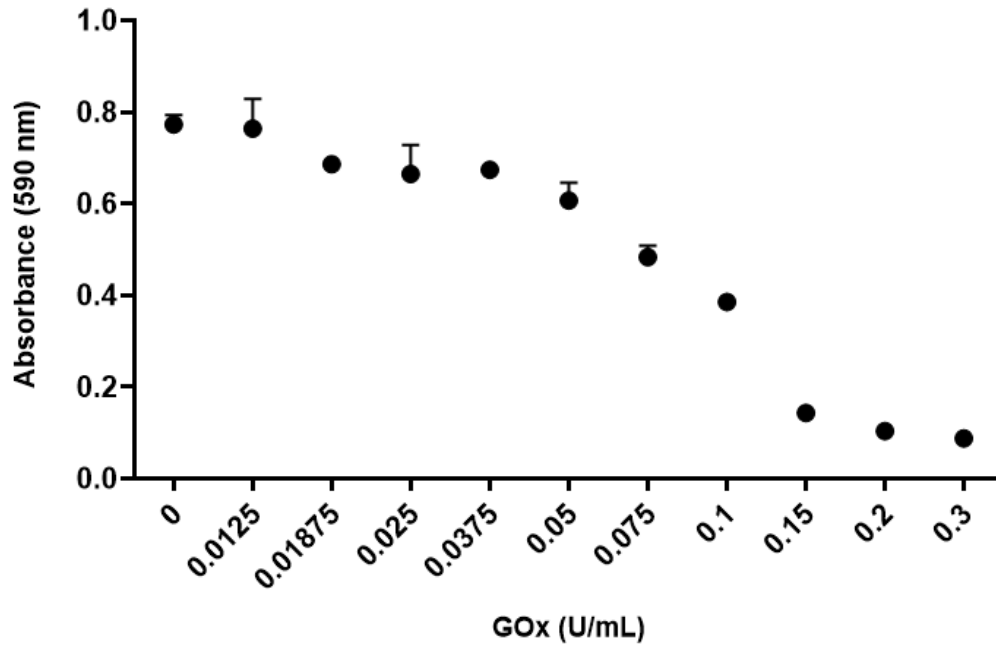
Figure 17: MTT cell viability assay of human U937 cells differentiated into macrophages and treated with different concentrations of GOx (0 to 0.3 U/mL) for 24 h. Mean values and SEM are indicated with bars.

The MTT cell viability assay of mouse RAW 264.7 macrophages treated with different concentrations of GOx (0 to 0.15 U/mL) for 24 h indicates that the RAW 264.7 cells begin undergoing cell death between 0 and 0.0094 U/mL GOx (Figure 18).
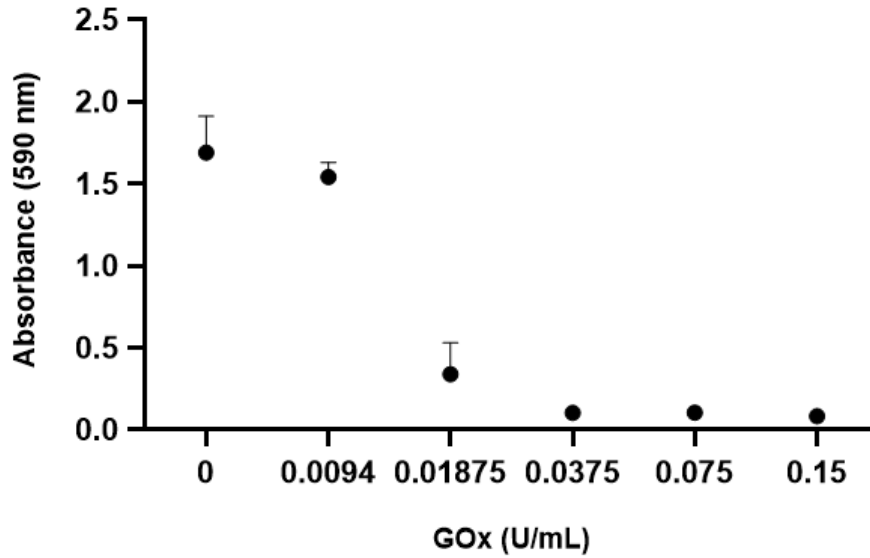
Figure 18: MTT cell viability assay of mouse RAW 264.7 macrophages treated with different concentrations of GOx (0 to 0.15 U/mL) for 24 h. Mean values and SEM are indicated with bars.

A second MTT cell viability assay of mouse RAW 264.7 macrophages treated with a lower concentration range of GOx (0 to 0.3 U/mL) for 24 h gives a more specific indication of the GOx level at which cells begin undergoing cell death, which is between 0.002 and 0.005 U/mL GOx (Figure 19).
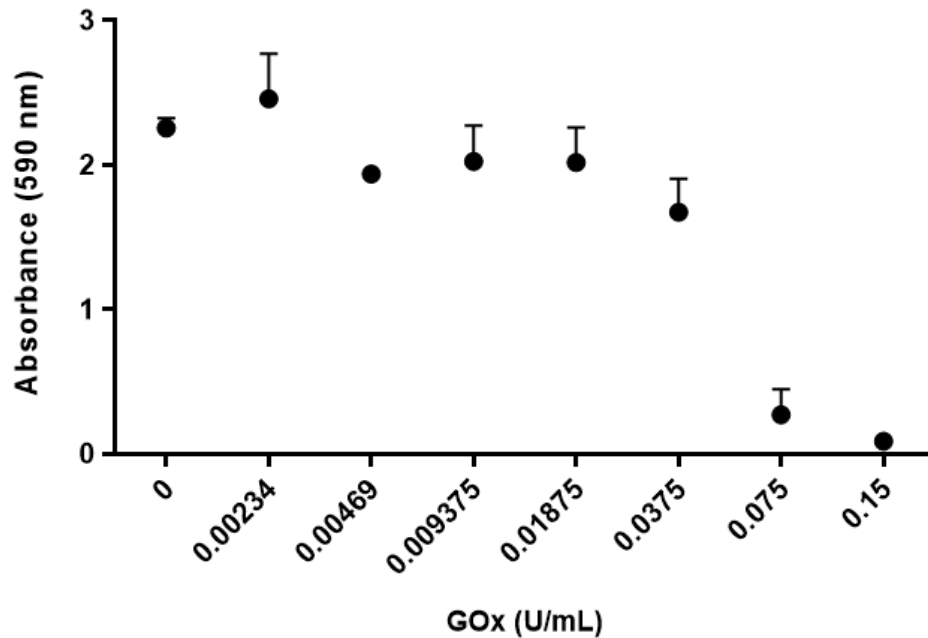
Figure 19: A second MTT cell viability assay of mouse RAW 264.7 macrophages treated with a lower concentration range of GOx (0 to 0.3 U/mL) for 24 h. Mean values and SEM are indicated with bars.

The MTT cell viability assay of mouse bone marrow derived macrophages (BMDMs) treated with different concentrations of GOx (0 to 0.15 U/mL) for 24 h indicates that the RAW 264.7 cells begin undergoing cell death between 0.002 and 0.005 U/mL GOx (Figure 20), similarly to the mouse RAW 264.7 macrophages. These BMDMs were obtained from mouse 5.C.2.
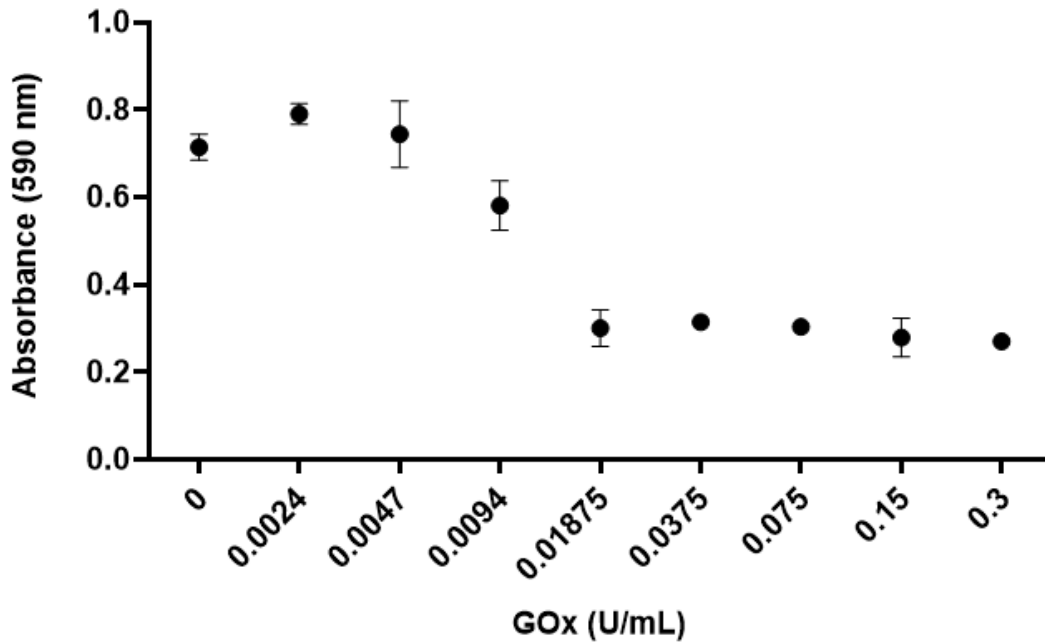
Figure 20: MTT cell viability assay of mouse bone marrow derived macrophages (BMDMs) treated with different concentrations of GOx (0 to 0.3 U/mL) for 24 h. Mean values and SEM are indicated with bars.

Once a nonlethal range of GOx concentrations at the threshold of lethality was established, these concentration ranges were used to treat the various cell types for 20-24 h, stimulate them with LPS and IFNγ, and measure the nitrite production of the macrophages through Griess reaction analysis.

For the second part of AIM II, we predicted that groups of progenitor cells that did and did not receive GOx treatment would yield significant differences in iNOS upregulation (i.e., nitrite production) after differentiation and stimulation (LPS + IFN-γ). Nitrite (and therefore indirectly NO) production was first measured in the human monocyte cells lines THP-1 and U937. Human cells were chosen as the initial cell models due to the more relevant comparisons that can be made between human cells and human sepsis patients than with murine cell lines.

THP-1 cells were seeded in flasks and either exposed to the GOx concentration ranges determined in part (1) or left untreated as controls. Both groups of cells were then differentiated into macrophages using PMA. A range of PMA concentrations were tested (0, 10, 20, 30, 50, and 100 ng/mL) in order to establish a level of PMA that induces differentiation of a large percentage of cells but does not affect iNOS upregulation in response to stimulation. The duration of time in which the monocytes were exposed to PMA was also varied (between 1 and 4 days) to further optimize a method for differentiating the cells while maintaining the iNOS upregulation stimulatory response (Figure 21).
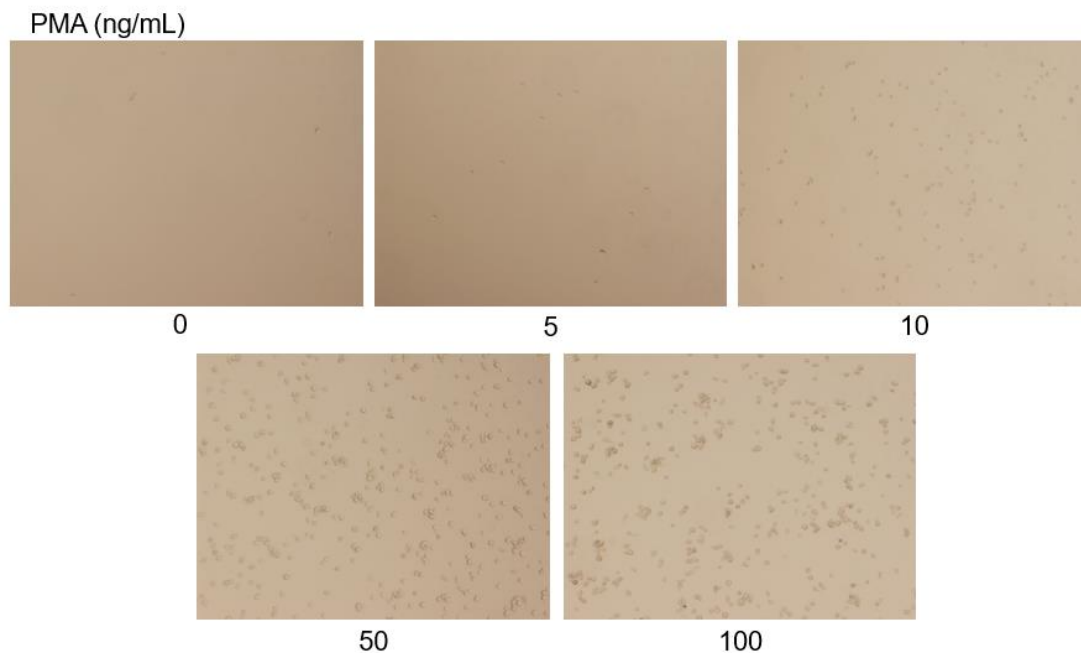
Figure 21: Representative microscope image of THP-1 monocytes differentiated with different concentrations of PMA (0 to 100 ng/mL) for a period of four days. Microscope images taken at 4x magnification.

As shown Figure 21, the normal plating density of 0.5-1.0x10^6 cells/mL was not sufficient to obtain high confluency of the differentiated macrophages using PMA. Therefore, much higher plating densities were used (4.0-6.0x10^6 cells/mL) for the subsequent Griess reaction assays. Representative microscope images of THP-1 cells treated with and without glucose oxidase (0.00625 U/mL) for 24 h then differentiated into macrophages with 30 ng/mL PMA for 24 h (Figure 22) and differentiated with 50 ng/mL for 3 days (Figure 23) show the confluency of THP-1 macrophages achieved by plating at these higher seeding densities.
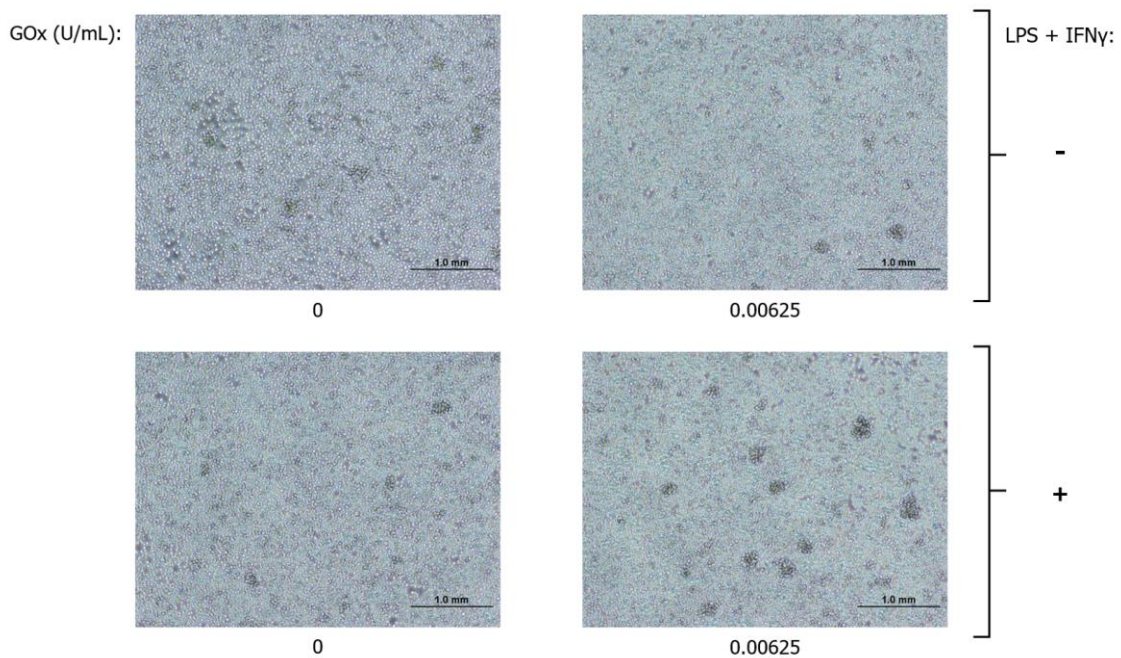
Figure 22: Representative microscope image of THP-1 cells treated with and without glucose oxidase (0.00625 U/mL) for 24 h then differentiated into macrophages with 30 ng/mL PMA for 24 h. At the time of imaging the cells were not yet stimulated. Microscope images were taken at a magnification of 4x.

GOx (U/mL):   0   0.00625
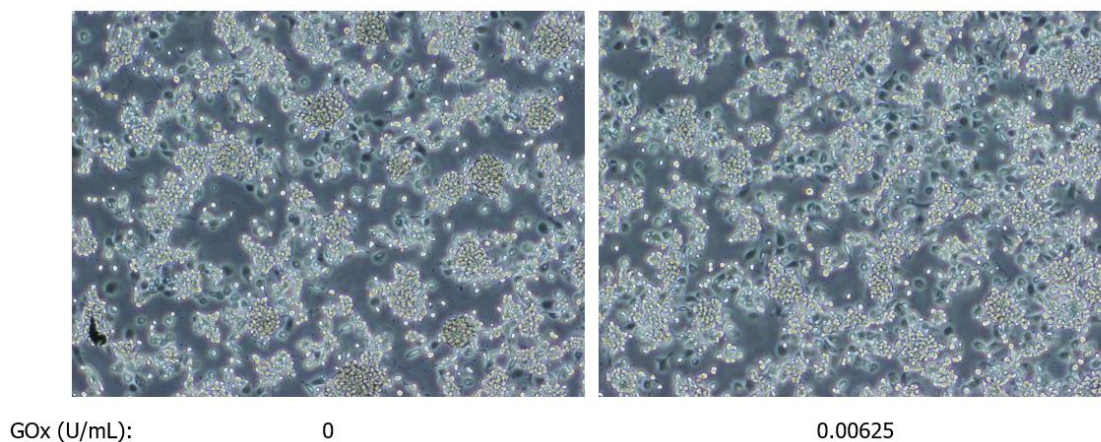
Figure 23: Representative microscope image of THP-1 cells treated with and without glucose oxidase (0.00625 U/mL) for 24 h then differentiated into macrophages with 50 ng/mL PMA for days. At the time of imaging the cells were not yet stimulated. Microscope images were taken at a magnification of 4x with the PhL filter.

Each group of stimulated or unstimulated THP-1 cells differentiated with various PMA concentrations for different amounts of time were stimulated with LPS + IFN-γ and assessed for nitrite production measurements via a Griess reaction assay. Many variables of the experiment were varied and assessed via Griess reaction assay: GOx concentrations, PMA concentrations (Figure 24), IFNγ concentrations (0 to 4,000 U/mL), duration of PMA treatment (1-4 days), and subsequent resting period duration (1-3 days). The nitrite produced by the differentiated THP-1 macrophages was extremely low for all combinations tested. Representative images of the nitrite production measured through Griess reaction assays show that the nitrite levels detected fall below the concentrations detected in the media-only wells in the standard nitrite curve and can therefore be considered negligible (Figure 25). None of the methods tested resulted in an acceptable positive control for iNOS upregulation.
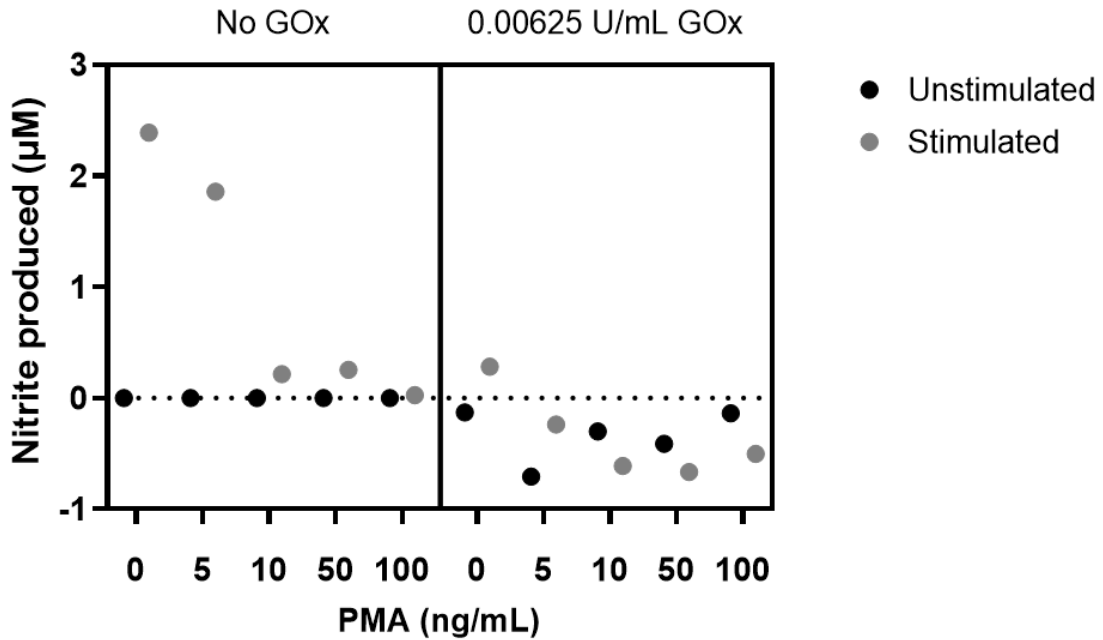
Figure 24: Representative nitrite production results of THP-1 cells treated with zero or 0.00625 U/mL GOx, differentiated into macrophages with different PMA concentrations, and stimulated (LPS + IFNγ) or unstimulated using Griess reaction assays.
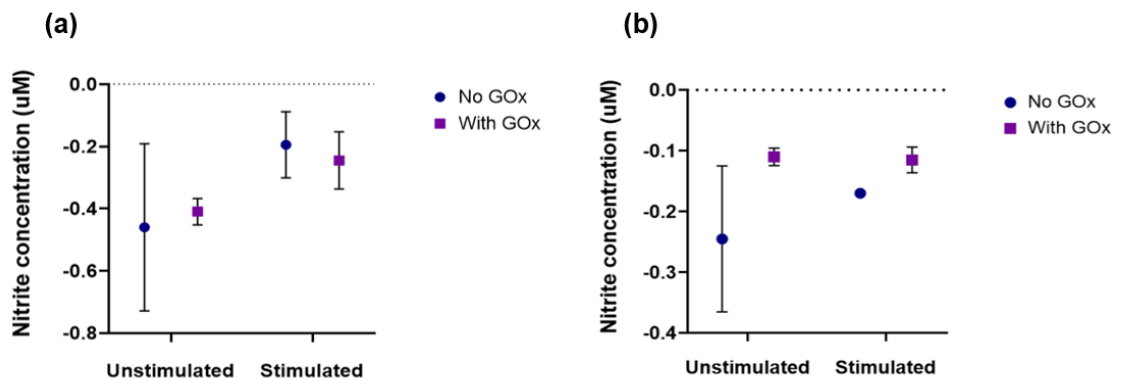
Figure 25: Representative nitrite production results of THP-1 cells treated with different concentrations of GOx, differentiated into macrophages with 30 ng/mL PMA, and stimulated (LPS + IFNγ) or unstimulated using Griess reaction assays. The GOx concentrations are (a) 0.00625 and (b) 0.009375 U/mL.

Next, the human monocyte U937 cell line was studied. While the U937 cells differentiated in different concentrations of PMA (30 and 50 ng/mL) and stimulated with LPS + IFNγ resulted in higher nitrite production levels than the THP-1 cells, the nitrite levels produced were low compared to the mouse BMDMs and did not result in distinguishable differences with different concentrations of GOx treatment (Figure 26, Figure 1Figure 27, and Figure 28).
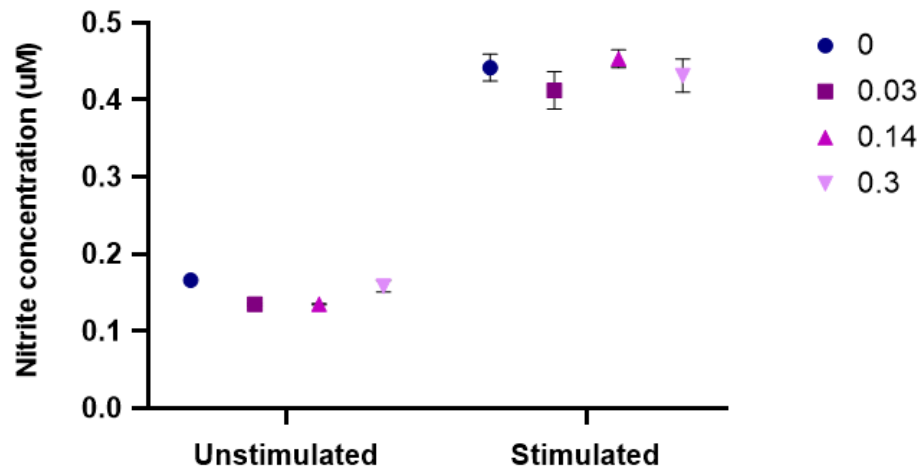
Figure 26: Nitrite production by human U937 macrophages treated with different concentrations of GOx (legend, 0 to 0.3 U/mL) and stimulated with LPS and IFNγ or left unstimulated. The U937 cells were differentiated into macrophages with 50 ng/mL PMA for 1 day, rested for 1 day, treated with different concentrations of GOx for 24 h, stimulated with LPS + IFNγ for 24 h, then the nitrite levels were assessed with a Griess reaction assay. Mean values with SEM are indicated by bars.
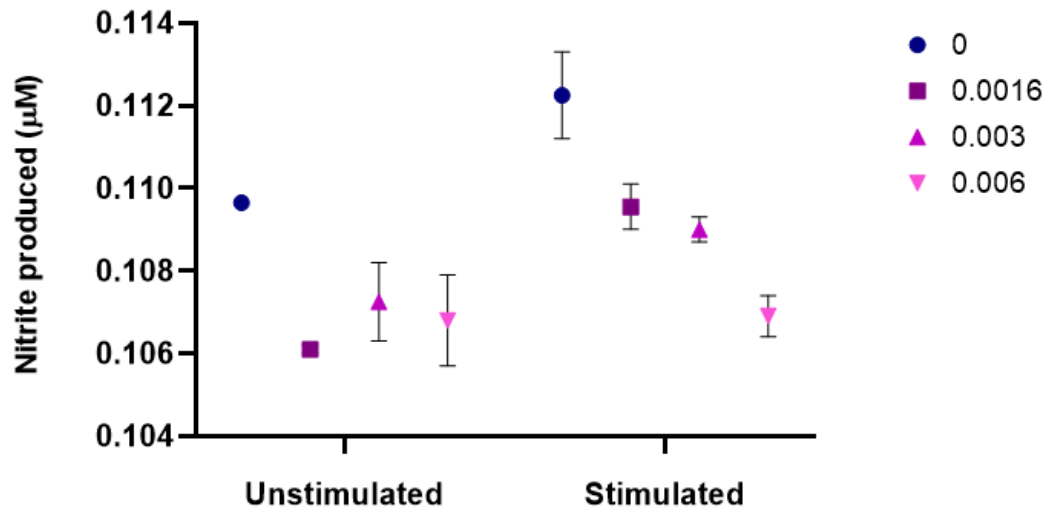
Figure 27: Griess reaction assay of U937 cells differentiated in 20 ng/mL PMA for one day, rested, and treated with different concentrations of GOx for 24 h. Two-way ANOVA analysis shows that the factors glucose oxidase (GOx) treatment ($F_{3,8} = 12.82$, $p < .01$) as well as stimulation with LPS + IFNγ ($F_{1,8} = 16.13$, $p < .01$) are significant. However, the interaction between GOx treatment and stimulation is not significant ($F_{3,8} = 2.11$, $p = 0.18$).
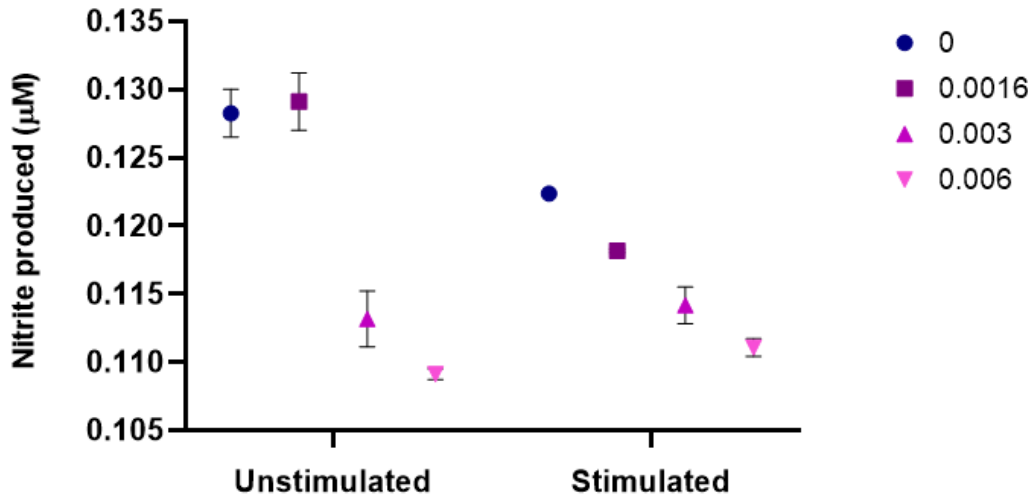
Figure 28: Griess reaction assay of U937 cells differentiated in 50 ng/mL PMA for one day, rested, and treated with different concentrations of GOx for 24 h. Two-way ANOVA analysis shows that the factors glucose oxidase (GOx) treatment ($F_{3,8} = 62.89$, $p < .0001$) as well as stimulation with LPS + IFNγ ($F_{1,8} = 13.68$, $p < .01$), as well as the interaction between GOx treatment and stimulation ($F_{3,8} = 10.50$, $p < .01$) are significant.

Microscope images of U937 cells treated with different concentrations of GOx, differentiated in 50 ng/mL PMA for one day, and rested for three days before stimulation with LPS + IFNγ (Figure 29 and Figure 30) show that increasing concentrations of GOx resulted in less viable macrophages at the end of the experiment. To assess whether the decrease in cell viability resulted in the dose response trends observed (Figure 27 and Figure 28), the nitrite production results were replotted as nitrite produced per gram of protein in each well. The cell samples were lysed and prepared as Western blot samples and protein content was determined via BCA analysis. Plots of µmol/g nitrite produced per gram of protein show the same trends as figures of non-normalized nitrite production (not shown due to low protein concentrations and negative µmol/g nitrite values).
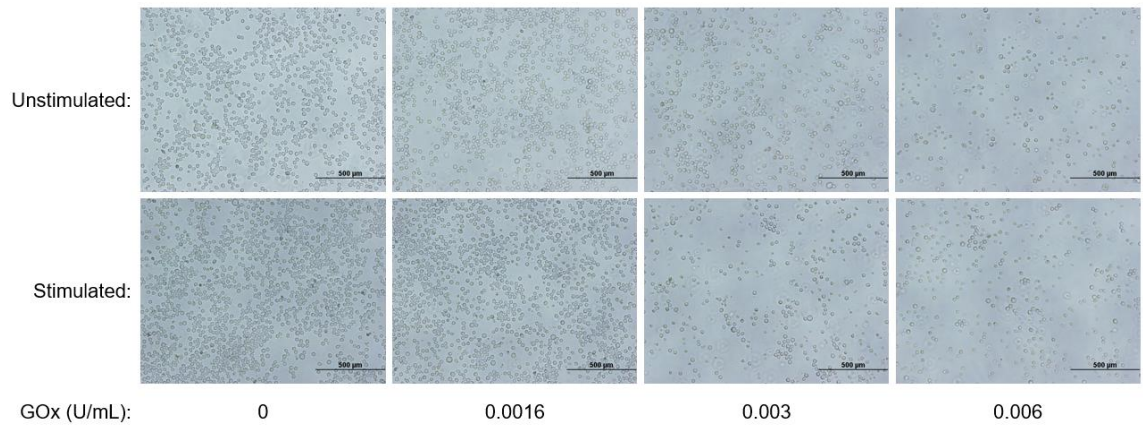
Figure 29: U937 cells treated with different concentrations of GOx (0 to 0.006 U/mL), differentiated in 20 ng/mL PMA for 1 day and rested for three days before stimulation.
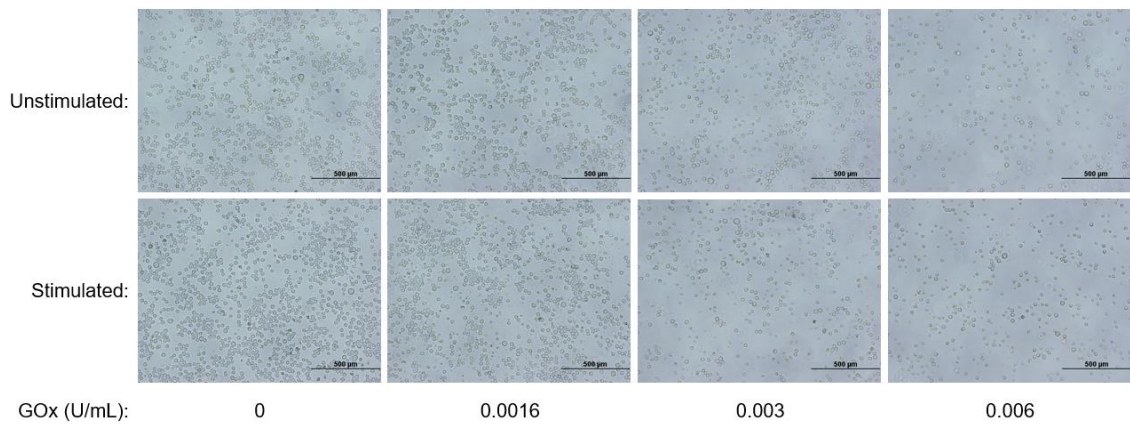
Figure 30: U937 cells treated with different concentrations of GOx (0 to 0.006 U/mL), differentiated in 50 ng/mL PMA for 1 day and rested for three days before stimulation.

Due to the lack of detected nitrite production in response to stimulation in differentiated THP-1 and U937 macrophages, bone marrow cells were isolated from aged, healthy mice and used for the GOx response experiment. The BM cells were rested for one day prior to treatment with different concentrations of GOx for 24 h. Cells were then differentiated into macrophages with LADMAC supernatant-containing media for 6-7 days, stimulated with LPS + IFNγ for 24 h, and nitrite production was detected with a

48

Griess reaction assay. The first experiment (mouse 5.C.1) resulted in an increased

production of nitrite by stimulated macrophages treated with 0 and 0.00625 U/mL GOx

(Figure 31). The downward trend in nitrite production in response to GOx concentration

is likely due to substantially lower viable cell numbers with increasing GOx concentrations

tested and not due to a cellular response.
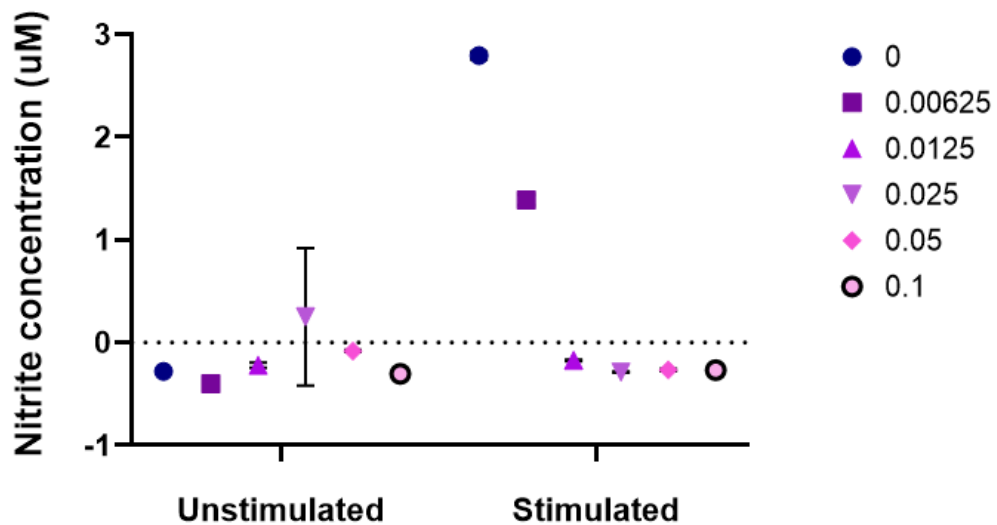
Figure 31: Nitrite produced by bone marrow derived macrophages (BMDMs) from an
aged control mouse (5.C.1) treated with different concentrations of glucose oxidase
(GOx) for 24 h. Pseudo-replicates are shown. The dose response trend seen in the
stimulated group is due to higher instances of cell death at the higher GOx concentrations
used.

Due to the vast loss of BMDM viability at GOx concentrations used initially, the

GOx concentrations were decreased by approximately ten-fold for a second experiment

with mouse BMDMs. The second experiment (mouse 5.C.2) was performed in the same

way as the first experiment, except that the concentration range of GOx treatments used

was between 0 and 0.003 U/mL (Figure 32). Duplicate measurements were taken from

each well of an unstimulated row of cells and also for one row of stimulated cells. These pseudo-replicates are graphed and are not true replicates.

These results indicate that the concentration of GOx treatment may have a significant effect on the nitrite production when the cells are stimulated versus unstimulated ($p < .001$, pseudo-replicates). A trend of increased nitrite production in response to stimulation for GOx concentrations of 0 to 0.0016 U/mL, followed by a decrease in nitrite production at the final GOx concentration tested, 0.003 U/mL is observed. Tukey *post hoc* analysis further indicates that differences in nitrite production between many of these GOx concentrations are significant, including the drop between 0.0016 and 0.003 U/mL ($p < .001$).
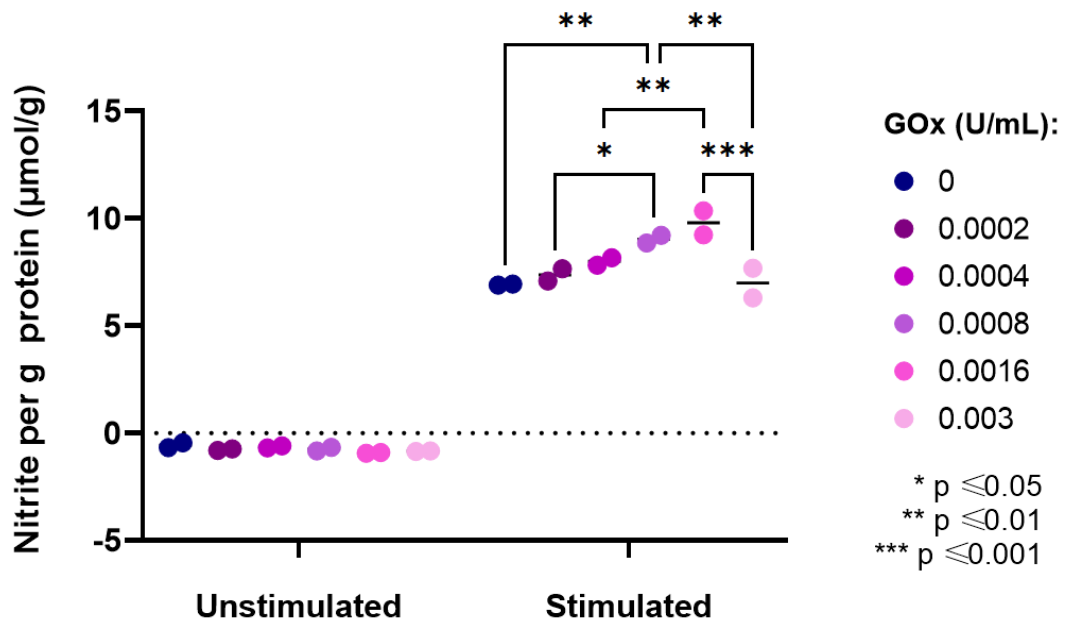
Figure 32: Nitrite production by aged control mouse (5.C.2) bone marrow derived macrophages (BMDMs) treated with different concentrations of GOx for 24 h and normalized to protein content. Duplicate measurements taken from each well. The mean nitrite production of the unstimulated cells was -0.75 mol/µg and the mean of the stimulated cells was 8.01 mol/µg. The concentration of GOx treatment does have an effect on the nitrite production when the cells are stimulated versus unstimulated and this effect is statistically significant ($F_{5,12} = 9.66$, $p < .001$).

The results obtained in the initial Griess reaction assay for mouse BM cells treated with GOx concentrations, washed, then differentiated for seven days (Figure 32) are normalized to protein content, which approximates normalization to cell count. Large percentages of the BMDMs remained viable after GOx treatment, washing, and differentiation into BMDMs even at the highest concentration tested (0.003 U/mL) as shown in Figure 33.

GOx (mU/mL):   LPS + IFNγ

| 0 | 0.2 | 0.4 | 0.8 | 1.6 | 3.0 |
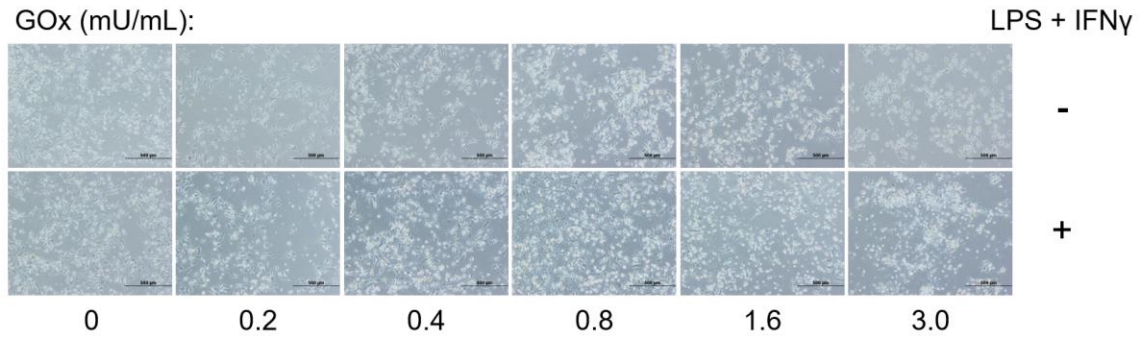
Figure 33: Microscope images of mouse BMDMs from an aged control mouse (5.C.2) used for Griess reaction analysis prior to LPS + IFNγ stimulation. BM cells were treated with different concentrations of glucose oxidase (GOx) for 24 h, washed, and differentiated into macrophages for seven days. Large percentages of BMDMs remain viable at the highest GOx concentration tested (0.003 U/mL). Magnification of 10x and scale bars represent a length of 500 μm.

To confirm the result of a trend in nitrite production in response to increased concentrations of GOx up to a certain threshold value (approximately 0.0016 U/mL in the mouse BMDMs) and a subsequent decrease in nitrite production at higher GOx concentrations obtained in mouse BMDMs, this experiment was repeated using mouse RAW 264.7 macrophages. The RAW 264.7 cells were treated with different concentrations of GOx (0 to 0.006 U/mL) for 24 h, differentiated into macrophages, and stimulated with LPS + IFNγ prior to measuring the nitrite production through Griess reaction assay analysis. The resultant nitrite values were normalized to cellular protein content to ensure any trends observed are not due to differences in numbers of viable cells between groups (Figure 34). The measurements obtained for the RAW 264.7 cells are pseudo-replicates ($n = 1$).

The mouse RAW 264.7 cells display a similar trend as the mouse BMDMs, where at low concentrations of GOx there is an increase in nitrite production up to a certain GOx

level (0.0016 U/mL for BMDMs and 0.003 U/mL for RAW 264.7 cells) and at the higher

GOx concentration tested the nitrite production falls. The mouse BMDMs appear to reach

a peak nitrite production at a lower GOx concentration than the RAW 264.7 cells,

potentially indicating that the mouse BMDMs are more susceptible to changes in iNOS

response due to oxidative GOx-induced stress than the mouse tumor RAW 264.7 cells.
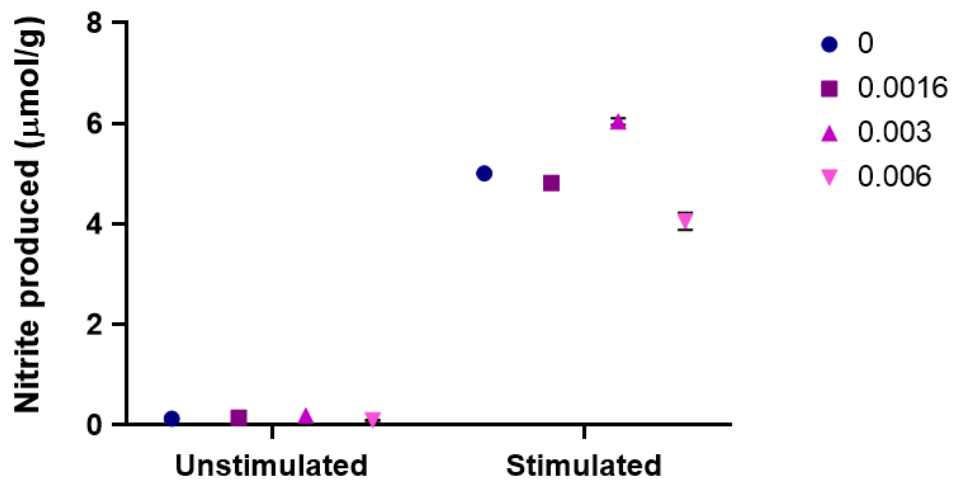
Figure 34: Nitrite production of mouse RAW 264.7 cells treated with different concentrations of GOx for 24 h, differentiated into macrophages, and stimulated with LPS and IFNγ, normalized to cellular protein content. Pseudo-replicate values of duplicate measurements from the same well plate are shown. Two-way ANOVA analysis shows that both factors glucose oxidase (GOx) treatment and stimulation with LPS + IFNγ as well as the interaction between them are significant ($F_{3,8} = 143.1$, $p <$ .0001). A post-hoc Tukey HSD test comparing all GOx concentration groups within stimulated and unstimulated groups shows no significant difference between any GOx concentration in the unstimulated group, but does show a significant difference between all other groups except between the 0 and 0.0016 U/mL GOx groups ($p < .0001$ for all other groups). Mean values and SEM are indicated by bars.

3.3 AIM III

The purpose of AIM III is to determine whether the suppression of iNOS

upregulation that was induced via oxidative stress (i.e. GOx) is associated with the DNA

damage response (DDR). Different cell types (mouse and human myeloid cells) were treated as described for AIM II. Briefly, cells were treated with the concentration range of GOx that induced the changes in nitrite production observed in AIM II for 24 h, differentiated into macrophages or left undifferentiated, stimulated (if differentiated) with LPS and IFNγ, and Western blot analysis was performed for activated DDR protein(s). We predicted that the concentration range of GOx that resulted in suppressed nitrite production in response to stimulation would result in a different amount of activated ATM (i.e. phosphorylated ATM, p-ATM).

Initial dot blot analysis of p-ATM and total ATM in undifferentiated RAW 264.7 cells treated with different concentrations of GOx for 24 h, treated with the GOx concentration range determined in AIM II (0 to 0.006 U/mL), show a significant positive correlation between pATM/total ATM (% pATM) and GOx treatment ($p < .05$) (Figure 35).
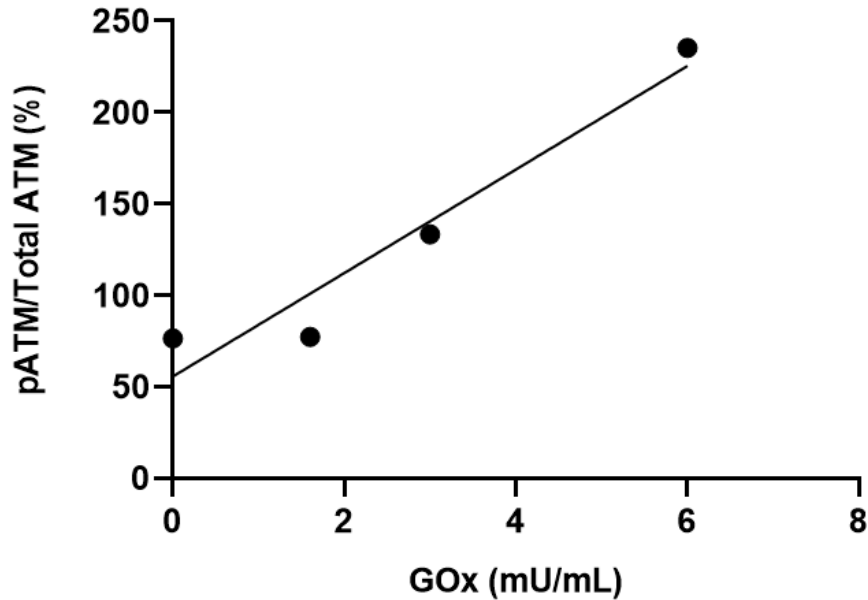
Figure 35: Preliminary phospho-ATM (p-ATM) dot blot analysis of undifferentiated RAW 264.7 cells treated with different concentrations of GOx (0, 0.0016, 0.003, and 0.006 U/mL) for 24 h. Pearson correlation analysis indicates a significant positive correlation between pATM/Total ATM (%) and GOx treatment ($r^2 = 0.93$, p = .03).

Western blot analysis of spleen lysate samples from mice in the mild and severe sepsis experiments were also performed to determine whether there are differences in expression of DDR proteins in spleen tissue at the time of euthanasia. All mice were euthanized within 12 hours of reaching the humane endpoint for non-survivors or three (mild) to seven (severe) days post-CLP sepsis surgery for survivors. No signal was obtained from the BMDM samples probed for various DDR proteins (p-ATM, ATM, p-CHK1, and CHK1). This is likely due to a Western blot preparation procedure that did not include extensive enough cell lysis methodology of the BMDMs. Western blotting of homogenized spleen tissue lysates resulted in no observable differences between controls or septic mice in iNOS expression for the mild and severe sepsis experiments. Blotting for phospho-Chk1 (p-Chk1) appears to have resulted in increased p-Chk1 in septic mice

compared to the controls in the mild sepsis experiment, but the results are inconclusive for

the severe sepsis experiment due to unequal protein loading as indicated by the total Chk1

protein (Figure 36).
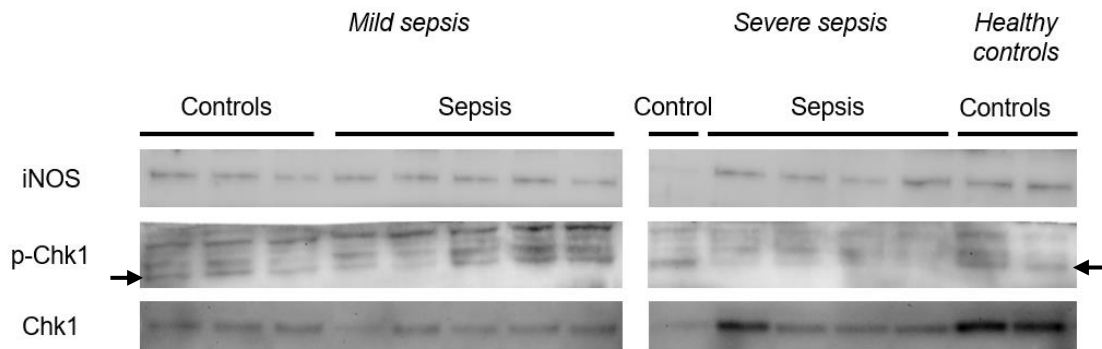
Figure 36: Western blots probing for iNOS, phosphorylated Chk1 (p-Chk1), and total Chk1 in homogenized mouse spleen lysates from the mild and severe sepsis experiments as well as two healthy control mice. The p-Chk1 band is indicated by arrows at approximately 55 kDa. The control and first (leftmost) sepsis mouse in the severe sepsis group and the two healthy controls are female. All other mice are male.

CHAPTER 4: DISCUSSION

AIM I

Mild sepsis experiment

In the mild sepsis experiment conducted under AIM I, differences in exhibition of the M1 phenotype between septic mice and healthy controls were explored. The first phenotype assessed for differential response was iNOS, which is regulated through transcriptional control of protein expression levels. Up-regulation was determined by two different methods, (1) iNOS protein expression levels through Western blot analysis and (2) nitric oxide (NO) production through a Griess reaction analysis.

Records of the sepsis scores and body temperatures from the mice in the mild sepsis experiment showed that the four survivors appeared healthy by several standard health assessment methods. The sepsis scores and body temperatures of the survivors returned to levels that were extremely similar to their control mouse cohorts. This finding is typical of human sepsis survivor patients, whose measurements by standard assessment tools for health (i.e., temperature, white blood cell count, etc.) usually return to healthy baseline levels even though the majority of sepsis survivors retain immunological suppression.

The nitrite production results from mildly septic BMDMs showed a significant decrease in nitrite production from stimulated (LPS + IFNγ) BMDMs compared to controls. This result was also reflected in Western blotting assessment of iNOS expression, where stimulated septic BMDMs showed less upregulation of iNOS than stimulated controls, with the exception of the single non-survivor. These results indicate that macrophages differentiated from bone marrow progenitor cells in mice that have experienced mild sepsis have a reduced ability to upregulate iNOS in response to

57

stimulation. Upregulation of iNOS is associated with the pro-inflammatory 'M1' macrophage phenotype, and this result may therefore indicate a suppressed ability of sepsis survivor macrophages to assume the M1 phenotype upon subsequent challenge.

Another indicator of macrophage phenotype studied is the presence of pseudopodia or protrusions from the cell body. Macrophages in the anti-inflammatory, repair-oriented 'M2' phenotypic state exhibit a greater number of pseudopodia than macrophages in the pro-inflammatory M1 state. The percentage of cells with pseudopodia was found to be different between stimulated and unstimulated control BMDMs in the mild sepsis experiment, but not in the septic group nor between controls and septic BMDMs. The significant trend indicates that the collection of non-septic BMDMs undergo a morphological change to include a lower percentage of cells exhibiting pseudopodia. This result may indicate that a larger percentage of unstimulated cells exhibit an M2 phenotype and undergo a morphological change to an M1 state upon stimulation, which is consistent with the view that macrophages can be 'classically activated' to take on the M1 phenotype by stimulation with LPS and IFNγ.

The septic group generally demonstrated much greater variability in the morphological pseudopodia exhibition response to stimulation. Interestingly, the BMDMs that displayed the opposite trend from the control group are from the non-survivor. This variability in disease group subjects is expected due to the highly complex nature of sepsis. However, with additional subjects in future studies, the opposite trend observed for the non-survivor may reveal an indicative maker of the susceptibility of mice to succumb to sepsis.

This morphological indicator of macrophage phenotype is consistent with the Griess reaction and Western blot results obtained for the mild sepsis experiment that indicate a polarization to the M1 phenotype upon stimulation for control cells, and an attenuated ability of BMDMs in the septic group to assume the M1 phenotype. All of the indicators tested for phenotypic differences (iNOS protein expression, NO production, and percentage of cells with pseudopodia) indicate that the cells from septic mice are hypo-responsive.

Severe sepsis experiment

The results of the severe sepsis experiment were complicated by the advanced age of the murine subjects and low number of BM cells obtained. However, the same trend of suppressed ability of stimulated septic BMDMs to produce nitrite compared to controls as seen in the mild sepsis experiment was again observed for the severely septic mice. These results support the hypothesis that septic mouse BMDMs are hypo-responsive to stimulation.

Measurements of differences in the phagocytic ability of severely septic BMDMs displayed trends indicating that in the control group, stimulated cells engulfed more 1-µm beads than unstimulated cells and in the septic group, stimulated cells engulfed fewer beads than unstimulated cells (p = ns). Data from the literature indicates that M2-polarized macrophages engulf more particles than M1-polarized macrophages. These results could indicate that either (1) the phagocytic ability of the macrophages conflicts with other evidence obtained in this study and the results in fact indicate that BMDMs of septic mice exhibit a greater ability to assume the M1 phenotype upon stimulation than controls, (2) the aged control BMDMs are in a more pro-inflammatory state than typical resting, healthy

59

macrophages and exhibit opposite behavior to what is expected by polarizing to a phagocytic state indicative of the M2 phenotype upon stimulation, (3) that septic BMDMs are not in either of the traditionally-held M1 or M2 states and exhibit an alternate phenotype in the polarization spectrum, (4) that differences between sub-phenotypes of the M2 phenotype are being observed. The results of bead phagocytosis studies are therefore inconclusive.

AIM II

The goal of AIM II was to determine a source of oxidative stress that would mimic the effects of sepsis in an *in vitro* cell model and result in a suppressed ability of macrophages to assume the M1 phenotype. Sublethal concentration ranges of GOx were chosen just below concentrations that caused a loss in cell viability, administered to macrophage progenitor cells, and the nitrite production of the stimulated, differentiated macrophages was measured. In both RAW 264.7 and BMDMs, a similar biphasic trend was observed where the nitrite production increases with increasing GOx concentration up to a certain threshold (0.0016 U/mL for BMDMs and 0.003 U/mL for RAW 264.7 cells), after which nitrite production falls. This may indicate that low amounts of oxidative stress cause macrophages to become pro-inflammatory, but at a certain sub-lethal threshold, suppression of NO production and M1 exhibition occurs in a dose-responsive manner. Mouse BMDMs appear to reach a peak nitrite production at a lower GOx concentration than the RAW 264.7 cells, potentially indicating that the mouse BMDMs are more susceptible to changes in iNOS response due to oxidative stress than the RAW 264.7 cells. These results support the hypothesis that a source of oxidative stress mimics the hypo-responsiveness of macrophages that is observed in septic macrophages.

AIM III

The goal of AIM III was to determine whether the suppression of iNOS upregulation that was induced via oxidative stress is associated with the DNA damage response (DDR). Different cell types (mouse and human myeloid cells) were treated with the sublethal GOx concentration range established in AIM II, differentiated into macrophages or left undifferentiated, stimulated (if differentiated) with LPS + IFNγ, and Western blot analysis was performed for activated DDR proteins.

Western blot analysis of spleen lysates from mice in the mild and severe sepsis experiments were also performed to determine whether there are differences in activation of DDR proteins in spleen tissue. Western blotting of homogenized spleen tissue lysates resulted in no observable differences in iNOS expression between controls or septic mice for mice in either the mild or severe sepsis experiments. However, results for activated Chk1 (p-Chk1) indicate increased Chk1 activation in septic mice compared to the controls in the mild sepsis experiment. This result supports the hypothesis that immune cells exhibit greater activation of DDR proteins during and after sepsis.

We found that RAW 264.7 cells treated with increasing concentrations of GOx (0 to 0.006 U/mL) exhibited increasing amounts of activated ATM (i.e., p-ATM). This result indicates that for the concentration ranges where a suppressed ability to upregulate iNOS was observed, there is also greater activation of the DDR ATM. A linear response was observed, which could either indicate that (1) the increasing concentrations of GOx led to increased amounts of DNA damage and subsequent activation of ATM, and/or (2) that the increasing concentrations of GOx activated the redox-sensing role of ATM, and/or (3) that the increasing concentrations of GOx activated ATM to initiate additional signal

transduction pathways that may lead to the epigenetic reprogramming of the cell to suppress iNOS upregulation. These results are therefore currently inconclusive, but may support the hypothesis that GOx may initiate similar epigenetic reprogramming events that occur in sepsis that lead to suppression of iNOS upregulation.

Taken as a whole these results demonstrate that bone marrow derived macrophages (BMDMs) from septic mice demonstrate a reduced ability to exhibit the pro-inflammatory 'M1' phenotype, as evidenced by attenuated iNOS protein expression and NO production in response to stimulation with LPS + IFNγ and changes in cell morphology. We have further determined that a specific concentration range of GOx may mimic this phenotypic hypo-responsiveness in BMDMs and RAW 264.7 cells and cause increased activation of DNA damage response (DDR) factor ATM. These results suggest a role for DDR factors in the macrophage immunosuppression that occurs in sepsis survivors.

REFERENCES

1. Singer, M.; Deutschman, C. S.; Seymour, C. W.; Shankar-Hari, M.; Annane, D.; Bauer, M.; Bellomo, R.; Bernard, G. R.; Chiche, J.-D.; Coopersmith, C. M.; Hotchkiss, R. S.; Levy, M. M.; Marshall, J. C.; Martin, G. S.; Opal, S. M.; Rubenfeld, G. D.; van der Poll, T.; Vincent, J.-L.; Angus, D. C., The Third International Consensus Definitions for Sepsis and Septic Shock (Sepsis-3). *JAMA* **2016,** *315* (8), 801-810.

2. CDC Sepsis: Data & Reports. https://www.cdc.gov/sepsis/datareports/index.html (accessed 16 August 2020).

3. Huang, M.; Cai, S.; Su, J., The Pathogenesis of Sepsis and Potential Therapeutic Targets. *International journal of molecular sciences* **2019,** *20* (21), 5376.

4. Cross, D.; Drury, R.; Hill, J.; Pollard, A. J., Epigenetics in Sepsis: Understanding Its Role in Endothelial Dysfunction, Immunosuppression, and Potential Therapeutics. *Frontiers in Immunology* **2019,** *10* (1363).

5. Boomer, J. S.; Green, J. M.; Hotchkiss, R. S., The changing immune system in sepsis: is individualized immuno-modulatory therapy the answer? *Virulence* **2014,** *5* (1), 45-56.

6. Arts, R. J.; Gresnigt, M. S.; Joosten, L. A.; Netea, M. G., Cellular metabolism of myeloid cells in sepsis. *J Leukoc Biol* **2017,** *101* (1), 151-164.

7. Cheng, S. C.; Scicluna, B. P.; Arts, R. J.; Gresnigt, M. S.; Lachmandas, E.;
    Giamarellos-Bourboulis, E. J.; Kox, M.; Manjeri, G. R.; Wagenaars, J. A.; Cremer, O.
    L.; Leentjens, J.; van der Meer, A. J.; van de Veerdonk, F. L.; Bonten, M. J.; Schultz,
    M. J.; Willems, P. H.; Pickkers, P.; Joosten, L. A.; van der Poll, T.; Netea, M. G.,
    Broad defects in the energy metabolism of leukocytes underlie immunoparalysis in
    sepsis. *Nat Immunol* **2016,** *17* (4), 406-13.

8. Rosenthal, M. D.; Moore, F. A., Persistent inflammatory, immunosuppressed,
    catabolic syndrome (PICS): A new phenotype of multiple organ failure. *Journal of
    advanced nutritional and human metabolism* **2015,** *1* (1), e784.

9. Wang, X.; Buechler, N. L.; Woodruff, A. G.; Long, D. L.; Zabalawi, M.; Yoza, B. K.;
    McCall, C. E.; Vachharajani, V., Sirtuins and Immuno-Metabolism of Sepsis. *Int J
    Mol Sci* **2018,** *19* (9).

10. Bomans, K.; Schenz, J.; Sztwiertnia, I.; Schaack, D.; Weigand, M. A.; Uhle, F.,
    Sepsis Induces a Long-Lasting State of Trained Immunity in Bone Marrow
    Monocytes. *Frontiers in immunology* **2018,** *9*, 2685-2685.

11. Irina; Jyue; Chittezhath, M.; Annelies; Beasley, F.; Hernández-Jiménez, E.; Toledano,
    V.; Cubillos-Zapata, C.; Rapisarda, A.; Chen, J.; Duan, K.; Yang, H.; Poidinger, M.;
    Melillo, G.; Nizet, V.; Arnalich, F.; López-Collazo, E.; Subhra, Human Monocytes
    Undergo Functional Re-programming during Sepsis Mediated by Hypoxia-Inducible
    Factor-1α. *Immunity* **2015,** *42* (3), 484-498.

12. Foster, S. L.; Hargreaves, D. C.; Medzhitov, R., Gene-specific control of
    inflammation by TLR-induced chromatin modifications. *Nature* **2007,** *447* (7147),
    972-978.

13. Yao, Y.; Xu, X.-H.; Jin, L., Macrophage Polarization in Physiological and Pathological Pregnancy. *Frontiers in immunology* **2019,** *10*, 792-792.

14. Arts, R. J. W.; Gresnigt, M. S.; Joosten, L. A. B.; Netea, M. G., Cellular metabolism of myeloid cells in sepsis. *Journal of Leukocyte Biology* **2017,** *101* (1), 151-164.

15. Leentjens, J.; Kox, M.; Van Der Hoeven, J. G.; Netea, M. G.; Pickkers, P., Immunotherapy for the Adjunctive Treatment of Sepsis: From Immunosuppression to Immunostimulation. Time for a Paradigm Change? *American Journal of Respiratory and Critical Care Medicine* **2013,** *187* (12), 1287-1293.

16. Bosmann, M.; Ward, P. A., The inflammatory response in sepsis. *Trends in Immunology* **2013,** *34* (3), 129-136.

17. Cheng, S.-C.; Scicluna, B. P.; Arts, R. J. W.; Gresnigt, M. S.; Lachmandas, E.; Giamarellos-Bourboulis, E. J.; Kox, M.; Manjeri, G. R.; Wagenaars, J. A. L.; Cremer, O. L.; Leentjens, J.; van der Meer, A. J.; van de Veerdonk, F. L.; Bonten, M. J.; Schultz, M. J.; Willems, P. H. G. M.; Pickkers, P.; Joosten, L. A. B.; van der Poll, T.; Netea, M. G., Broad defects in the energy metabolism of leukocytes underlie immunoparalysis in sepsis. *Nat Immunol* **2016,** *17* (4), 406-413.

18. Butcher, S. K.; O'Carroll, C. E.; Wells, C. A.; Carmody, R. J., Toll-Like Receptors Drive Specific Patterns of Tolerance and Training on Restimulation of Macrophages. *Frontiers in immunology* **2018,** *9*, 933-933.

19. Fernández-Morera, J. L.; Calvanese, V.; Rodríguez-Rodero, S.; Menéndez-Torre, E.; Fraga, M. F., Epigenetic regulation of the immune system in health and disease. *Tissue Antigens* **2010,** *76* (6), 431-439.

20. Busslinger, M.; Tarakhovsky, A., Epigenetic control of immunity. *Cold Spring Harbor perspectives in biology* **2014,** *6* (6), a019307.

21. Seeley, J. J.; Baker, R. G.; Mohamed, G.; Bruns, T.; Hayden, M. S.; Deshmukh, S. D.; Freedberg, D. E.; Ghosh, S., Induction of innate immune memory via microRNA targeting of chromatin remodelling factors. *Nature* **2018,** *559* (7712), 114-119.

22. Beltrán-García, J.; Osca-Verdegal, R.; Romá-Mateo, C.; Carbonell, N.; Ferreres, J.; Rodríguez, M.; Mulet, S.; García-López, E.; Pallardó, F. V.; García-Giménez, J. L., Epigenetic biomarkers for human sepsis and septic shock: insights from immunosuppression. *Epigenomics* **2020,** *12* (7), 617-646.

23. Davis, F. M.; Gallagher, K. A., Epigenetic Mechanisms in Monocytes/Macrophages Regulate Inflammation in Cardiometabolic and Vascular Disease. *Arteriosclerosis, Thrombosis, and Vascular Biology* **2019,** *39* (4), 623-634.

24. Roy, D. G.; Chen, J.; Mamane, V.; Ma, E. H.; Muhire, B. M.; Sheldon, R. D.; Shorstova, T.; Koning, R.; Johnson, R. M.; Esaulova, E.; Williams, K. S.; Hayes, S.; Steadman, M.; Samborska, B.; Swain, A.; Daigneault, A.; Chubukov, V.; Roddy, T. P.; Foulkes, W.; Pospisilik, J. A.; Bourgeois-Daigneault, M.-C.; Artyomov, M. N.; Witcher, M.; Krawczyk, C. M.; Larochelle, C.; Jones, R. G., Methionine Metabolism Shapes T Helper Cell Responses through Regulation of Epigenetic Reprogramming. *Cell Metabolism* **2020,** *31* (2), 250-266.e9.

25. Carsten Carlberg, F. M., *Human Epigenetics: How Science Works*. 1 ed.; Springer International Publishing: 2019.

26. Weiterer, S.; Uhle, F.; Lichtenstern, C.; Siegler, B. H.; Bhuju, S.; Jarek, M.; Bartkuhn, M.; Weigand, M. A., Sepsis induces specific changes in histone modification patterns in human monocytes. *PloS one* **2015,** *10* (3), e0121748-e0121748.

27. Chan, G. C.; Fish, J. E.; Mawji, I. A.; Leung, D. D.; Rachlis, A. C.; Marsden, P. A., Epigenetic Basis for the Transcriptional Hyporesponsiveness of the Human Inducible Nitric Oxide Synthase Gene in Vascular Endothelial Cells. *The Journal of Immunology* **2005,** *175* (6), 3846-3861.

28. de Andrés, M. C.; Imagawa, K.; Hashimoto, K.; Gonzalez, A.; Roach, H. I.; Goldring, M. B.; Oreffo, R. O. C., Loss of methylation in CpG sites in the NF-κB enhancer elements of inducible nitric oxide synthase is responsible for gene induction in human articular chondrocytes. *Arthritis & Rheumatism* **2013,** *65* (3), 732-742.

29. Danielski, L. G.; Giustina, A. D.; Bonfante, S.; Barichello, T.; Petronilho, F., The NLRP3 Inflammasome and Its Role in Sepsis Development. *Inflammation* **2020,** *43* (1), 24-31.

30. Ahmad, A.; Vieira, J. d. C.; de Mello, A. H.; de Lima, T. M.; Ariga, S. K.; Barbeiro, D. F.; Barbeiro, H. V.; Szczesny, B.; Törö, G.; Druzhyna, N.; Randi, E. B.; Marcatti, M.; Toliver-Kinsky, T.; Kiss, A.; Liaudet, L.; Salomao, R.; Soriano, F. G.; Szabo, C., The PARP inhibitor olaparib exerts beneficial effects in mice subjected to cecal ligature and puncture and in cells subjected to oxidative stress without impairing DNA integrity: A potential opportunity for repurposing a clinically used oncological drug for the experimental therapy of sepsis. *Pharmacological Research* **2019,** *145*, 104263.

31. Figueiredo, N.; Chora, A.; Raquel, H.; Pejanovic, N.; Pereira, P.; Hartleben, B.; Neves-Costa, A.; Moita, C.; Pedroso, D.; Pinto, A.; Marques, S.; Faridi, H.; Costa, P.; Gozzelino, R.; Zhao, Jimmy L.; Soares, Miguel P.; Gama-Carvalho, M.; Martinez, J.; Zhang, Q.; Döring, G.; Grompe, M.; Simas, J. P.; Huber, Tobias B.; Baltimore, D.; Gupta, V.; Green, Douglas R.; Ferreira, João A.; Moita, Luis F., Anthracyclines Induce DNA Damage Response-Mediated Protection against Severe Sepsis. *Immunity* **2013,** *39* (5), 874-884.

32. Aguilar-Quesada, R.; Muñoz-Gámez, J. A.; Martín-Oliva, D.; Peralta, A.; Valenzuela, M. T.; Matínez-Romero, R.; Quiles-Pérez, R.; Murcia, J. M.-d.; de Murcia, G.; de Almodóvar, M. R.; Oliver, F. J., Interaction between ATM and PARP-1 in response to DNA damage and sensitization of ATM deficient cells through PARP inhibition. *BMC Molecular Biology* **2007,** *8* (1), 29.

33. Weintz, G.; Olsen, J. V.; Frühauf, K.; Niedzielska, M.; Amit, I.; Jantsch, J.; Mages, J.; Frech, C.; Dölken, L.; Mann, M.; Lang, R., The phosphoproteome of toll-like receptor-activated macrophages. *Molecular systems biology* **2010,** *6*, 371-371.

34. Chatzinikolaou, G.; Karakasilioti, I.; Garinis, G. A., DNA damage and innate immunity: links and trade-offs. *Trends in Immunology* **2014,** *35* (9), 429-435.

35. Neves-Costa, A.; Moita, L. F., Modulation of inflammation and disease tolerance by DNA damage response pathways. *The FEBS Journal* **2017,** *284* (5), 680-698.

36. Houtgraaf, J. H.; Versmissen, J.; van der Giessen, W. J., A concise review of DNA damage checkpoints and repair in mammalian cells. *Cardiovascular Revascularization Medicine* **2006,** *7* (3), 165-172.

37. Ditch, S.; Paull, T. T., The ATM protein kinase and cellular redox signaling: beyond the DNA damage response. *Trends in Biochemical Sciences* **2012,** *37* (1), 15-22.

38. Hotokezaka, Y.; Katayama, I.; Nakamura, T., ATM-associated signalling triggers the unfolded protein response and cell death in response to stress. *Communications Biology* **2020,** *3* (1), 378.

39. Valentin-Vega, Y. A.; Kastan, M. B., A new role for ATM. *Autophagy* **2012,** *8* (5), 840-841.

40. Ito, K.; Hirao, A.; Arai, F.; Matsuoka, S.; Takubo, K.; Hamaguchi, I.; Nomiyama, K.; Hosokawa, K.; Sakurada, K.; Nakagata, N.; Ikeda, Y.; Mak, T. W.; Suda, T., Regulation of oxidative stress by ATM is required for self-renewal of haematopoietic stem cells. *Nature* **2004,** *431* (7011), 997-1002.

41. Dejager, L.; Pinheiro, I.; Dejonckheere, E.; Libert, C., Cecal ligation and puncture: the gold standard model for polymicrobial sepsis? *Trends in Microbiology* **2011,** *19* (4), 198-208.

42. Rittirsch, D.; Huber-Lang, M. S.; Flierl, M. A.; Ward, P. A., Immunodesign of experimental sepsis by cecal ligation and puncture. *Nature Protocols* **2009,** *4* (1), 31-36.

43. Xu, W.-C.; Dong, X.; Ding, J.-L.; Liu, J.-C.; Xu, J.-J.; Tang, Y.-H.; Yi, Y.-P.; Lu, C.; Yang, W.; Yang, J.-S.; Gong, Y.; Zhou, J.-L., Nanotubular TiO$_2$ regulates macrophage M2 polarization and increases macrophage secretion of VEGF to accelerate endothelialization via the ERK1/2 and PI3K/AKT pathways. *International Journal of Nanomedicine* **2019,** *Volume 14*, 441-455.

44. Schliefsteiner, C.; Ibesich, S.; Wadsack, C., Placental Hofbauer Cell Polarization Resists Inflammatory Cues In Vitro. *International Journal of Molecular Sciences* **2020,** *21* (3), 736.

45. Luthria, G.; Li, R.; Wang, S.; Prytyskach, M.; Kohler, R. H.; Lauffenburger, D. A.; Mitchison, T. J.; Weissleder, R.; Miller, M. A., In vivo microscopy reveals macrophage polarization locally promotes coherent microtubule dynamics in migrating cancer cells. *Nature Communications* **2020,** *11* (1).

46. Kapellos, T. S.; Taylor, L.; Lee, H.; Cowley, S. A.; James, W. S.; Iqbal, A. J.; Greaves, D. R., A novel real time imaging platform to quantify macrophage phagocytosis. *Biochemical Pharmacology* **2016,** *116*, 107-119.

47. Panayiotidis, M.; Tsolas, O.; Galaris, D., Glucose oxidase-produced H2O2 induces Ca2+-dependent DNA damage in human peripheral blood lymphocytes. *Free Radic Biol Med* **1999,** *26* (5-6), 548-56.